EXISTENCE AND STABILITY OF STANDING PULSES IN NEURAL NETWORKS: II. STABILITY

YIXIN GUO* AND CARSON C. CHOW†

Abstract. We analyze the stability of standing pulse solutions of a neural network integro-differential equation. The network consists of a coarse-grained layer of neurons synaptically connected by lateral inhibition with a non-saturating nonlinear gain function. When two standing single-pulse solutions coexist, the small pulse is unstable, and the large pulse is stable. The large single-pulse is bistable with the "all-off" state. This bistable localized activity may have strong implications for the mechanism underlying working memory. We show that dimple pulses have similar stability properties to large pulses but double pulses are unstable.

Key words. integro-differential equations, integral equations, standing pulses, neural networks, stability

AMS subject classifications. 34A36, 37N25, 45G10, 92B20

1. Introduction. In the accompanying paper [25], we considered stationary localized self-sustaining solutions of an integro-differential neural network or neural field equation. The pulses are bistable with an inactive neural state and could be the underlying mechanism of persistent neuronal activity responsible for working memory. However, in order to serve as a memory, these states must be stable to perturbations. Here we compute the linear stability of stationary pulse states.

The neural field equation has the form

$$\frac{\partial u(x,t)}{\partial t} + u(x,t) = \int_{-\infty}^{\infty} w(x-y) f[u(y)] dy \tag{1.1}$$

with a nonsaturating gain function

$$f[u] = [\alpha(u(y,t) - u_T) + 1]\Theta(u - u_T) \tag{1.2}$$

where $\Theta(\cdot)$ is the Heaviside function, and "wizard hat" connection function

$$w(x) = Ae^{-a|x|} - e^{-|x|}. \tag{1.3}$$

In Ref [25], we considered stationary solutions $u_0(x)$, where $u_0(x) > u_T$ on an interval $-x_T < x < x_T$, $u(x_T, t) = u_T$, and $u(x,t) = u_0(x)$ satisfies the stationary integral equation

$$u_0(x) = \int_{-x_T}^{x_T} w(x-y)[\alpha(u_0(y) - u_T) + 1] dy, \tag{1.4}$$

We have shown the existence of pulse solutions of equation (1.4) in the form of single-pulses, dimple pulses and double pulses [24, 25]. Examples can be seen in Figs. 1.1, 7.1 and 6.1. We constructed the pulses by converting the integral equation (1.4) into piecewise-linear ODEs and then matching their solutions at the threshold points x_T. When the excitation A and gain α is small, there are no pulse solutions. If either

*Department of Mathematics, The Ohio State University, Columbus, OH 43210 (yigst@math.ohio-state.edu).

†Department of Mathematics, University of Pittsburgh, Pittsburgh, PA 15260 (ccchow@pitt.edu).

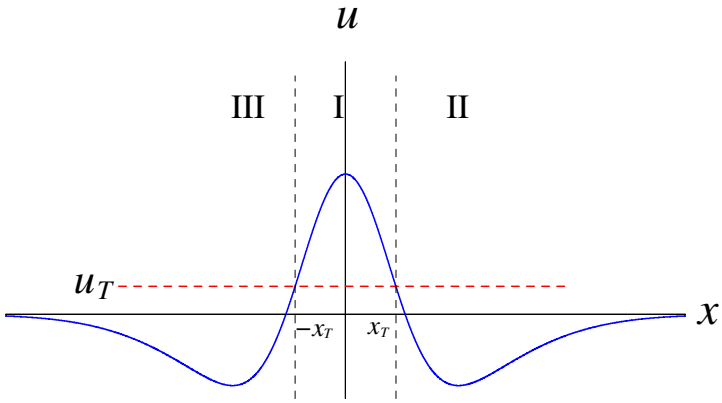

FIG. 1.1. *Single-pulse solution.*

is increased, there is a saddle-node bifurcation where two coexisting single-pulses, a small one and a large one, arise. As the gain or excitation increases, more than two pulses can coexist. For certain parameters, the large pulse can become a dimple pulse, and a dimple pulse can become a double pulse [24, 25].

In this paper, we derive an eigenvalue equation to analyze the stability of the pulse solutions. While our eigenvalue equation is valid for any continuous and integrable connection function $w(x)$, we explicitly compute the eigenvalues for (1.3). For the cases that we tested, we find that the small pulse is unstable and the large pulse is stable. If there is a third (larger) pulse then it is unstable. The stability properties of dimple pulses are the same as corresponding large pulses. Double pulses are unstable.

2. Eigenvalue equation for stability. We consider small perturbations around a stationary pulse solution by substituting $u(x,t) = u_0(x) + \epsilon v(x,t)$ into (1.1), where $\epsilon > 0$ is small. Since the pulse solutions are localized in space, we must assume the perturbation to the pulse will lead to time dependent changes to the boundaries of the stationary pulse (i.e where $u_0(x_T) = u_T$). Thus the boundaries $-x_T$ and x_T become time dependent functions

$$x_1(t) = -x_T + \epsilon\Delta_1(t) \tag{2.1}$$

$$x_2(t) = x_T + \epsilon\Delta_2(t) \tag{2.2}$$

where $\epsilon\Delta_1(t)$ and $\epsilon\Delta_2(t)$ are the changes of the boundaries $-x_T$ and x_T produced by the small perturbations. Inserting $u(x,t) = u_0(x) + \epsilon v(x,t)$ into (1.1) and eliminating the stationary solution with (1.4) gives

$$v_t(x,t) + v(x,t) = \alpha \int_{-x_T}^{x_T} w(x-y)v(y,t)dy + I_1 + I_2 \tag{2.3}$$

where

$$I_1 = \int_{-(x_T+\epsilon\Delta_1(t))}^{-x_T} w(x-y)[\alpha(u_0(y) + \epsilon v(y,t) - u_T) + 1]dy, \tag{2.4}$$

$$I_2 = \int_{x_T}^{x_T+\epsilon\Delta_2(t)} w(x-y)[\alpha(u_0(y) + \epsilon v(y,t) - u_T) + 1]dy. \tag{2.5}$$

Expanding the integrals I_1 and I_2 to order ϵ yields the linearized dynamics for the perturbations $v(x,t)$

$$v_t(x,t) + v(x,t) = \alpha \int_{-x_T}^{x_T} w(x-y)v(y,t)dy - w(x+x_T)\Delta_1 + w(x-x_T)\Delta_2. \tag{2.6}$$

The time dependence of Δ_1 and Δ_2 is found by using the fact that $u(x,t)$ is equal to the threshold u_T at the boundaries of the pulse. Inserting (2.1) and (2.2) into the boundary condition $u(x_1(t),t) = u_T$ and expanding to first order in ϵ leads to

$$\Delta_1(t) = -\frac{v(-x_T,t)}{c} \tag{2.7}$$

where

$$c = \left.\frac{du_0(x)}{dx}\right|_{x=-x_T} > 0. \tag{2.8}$$

Similarly,

$$\Delta_2(t) = \frac{v(x_T,t)}{c}. \tag{2.9}$$

Consider time variations of $v(x,t)$ that obey

$$v(x,t) = v(x)e^{\lambda t} \tag{2.10}$$

where $v(x)$ is a bounded and continuous function that decays to 0 exponentially as $x \to \pm\infty$. Substitute (2.10) with (2.7) and (2.9) into (2.6), to obtain

$$(1+\lambda)v(x) = w(x-x_T)\frac{v(x_T)}{c} + w(x+x_T)\frac{v(-x_T)}{c} + \alpha \int_{-x_T}^{x_T} w(x-y)v(y)dy. \tag{2.11}$$

where λ is an eigenvalue with corresponding eigenfunction $v(x)$. Equation (2.11) is an eigenvalue problem that governs the stability of small perturbations to pulse solutions of the neural field equation (1.1). If the real parts of all the eigenvalues are negative, the stationary pulse solution $u_0(x)$ is stable. If the real part of one of the eigenvalues is positive, $u_0(x)$ is unstable.

We define an operator L: $C[-x_T,x_T] \to C[-x_T,x_T]$:

$$Lv(x) = w(x-x_T)\frac{v(x_T)}{c} + w(x+x_T)\frac{v(-x_T)}{c} + \alpha \int_{-x_T}^{x_T} w(x-y)v(y)dy. \tag{2.12}$$

Then the eigenvalue equation (2.11) becomes

$$(1+\lambda)v(x) = L(v(x)) \qquad \text{on} \quad C[-x_T,x_T]. \tag{2.13}$$

We show in the Appendix (Theorem 8.7) that L is a compact operator. We also show the following properties of the eigenvalue equation (2.11):

1. Eigenvalues λ are always real (Theorem 8.4).
2. Eigenvalues λ are bounded by $\lambda_b \equiv \frac{2k_0}{c} + 2\alpha k_1 x_T - 1$ where k_0 is the maximum of $|w(x)|$ on $[0,2x_T]$ and $|w(x-y)| \le k_1$ for all $(x,y) \in J \times J$, $J = [-x_T,x_T]$ (Theorem 8.5).

3. Zero is always an eigenvalue (Theorem 8.6).
4. $\lambda = -1$ is the only possible accumulation point of the eigenvalues (Theorem 8.8). Thus, the only possible essential spectrum of operator L is located at $\lambda = -1$ implying that the discrete spectrum of L (i.e. eigenvalues of (2.11)) captures all of the stability properties.

We use these properties to compute the discrete eigenvalues to determine stability of the pulse solutions.

3. Linear stability analysis of the Amari case ($\alpha = 0$). Amari [3] computed the stability of pulse solutions to (1.1) for $\alpha = 0$. He obtained stability by computing the dynamics of the pulse boundary points. He found that the small pulse is always unstable and the large pulse is always stable. Pinto and Ermentrout [43] later confirmed Amari's results by deriving an eigenvalue problem for small perturbations.

We consider a stationary pulse solution of (1.1) with width x_T. Applying eigenvalue equation (2.11) to the Amari case yields

$$(1+\lambda)v(x) = w(x-x_T)\frac{v(x_T)}{c} + w(x+x_T)\frac{v(-x_T)}{c} \equiv T_1(v(x)), \tag{3.1}$$

where T_1 is a compact operator on $C[-x_T, x_T]$ (see Theorem 8.7). The spectrum of a compact operator is a countable set with no accumulation point different from zero. Therefore, the only possible location of the essential spectrum for T_1 is at $\lambda = -1$. This implies that instability of a pulse is indicated by the existence of a positive discrete eigenvalue.

The eigenvalue λ can be obtained by setting $x = -x_T$ and $x = x_T$ in (3.1) to give a two dimensional system

$$\left(1+\lambda-\frac{w(0)}{c}\right)v(x_T) - \frac{w(2x_T)}{c}v(-x_T) = 0 \tag{3.2}$$

$$-\frac{w(2x_T)}{c}v(x_T) + \left(1+\lambda-\frac{w(0)}{c}\right)v(-x_T) = 0 \tag{3.3}$$

This is identical to the eigenvalue equation of Ref [43]. Setting the determinant of system (3.2) and (3.3) to zero gives the eigenvalues

$$\lambda = \frac{w(0) \pm w(2x_T)}{c} - 1, \tag{3.4}$$

which agrees with Ref. [43].

The stationary solution of the Amari problem satisfies

$$u(x) = \int_{-x_T}^{x_T} w(x-y)dy = \int_{x+x_T}^{x-x_T} w(y)dy \tag{3.5}$$

Differentiating $u(x)$ yields $u'(x) = w(x+x_T) - w(x-x_T)$ implying

$$u'(-x_T) = w(0) - w(2x_T) = c. \tag{3.6}$$

Inserting into (3.4) gives the eigenvalues

$$\lambda = \frac{w(0) + w(2x_T)}{c} - 1, \quad 0 \tag{3.7}$$

The zero eigenvalue was expected from translational symmetry. Since $w(0) > w(2x_T)$, the sign of c alone determines stability of the pulse. Recall that the small and large pulse arise from a saddle node bifurcation [3, 24, 25]. At the saddle node bifurcation, both eigenvalues are zero. Thus, setting $\lambda = 0$ in (3.7) shows that the width of the pulse satisfies $w(2x_T) = 0$ [3]. For our connection function, $w(x)$ has only one zero at x_0 for $w(x)$ on $(0, \infty)$ (see [24, 25]). Thus $x_T = x_0/2$ at the saddle node. For the large pulse, $x_T > x_0/2$, implying $w(2x_T) < 0$ and $c > 0$. Conversely, $c < 0$ for the small pulse. Thus the large pulse is stable and small pulse is unstable.

Consider the example: $a = 2.4$, $A = 2.8$, $u_T = 0.400273$, $\alpha = 0$. There exist two single-pulses, the large pulse **l** and the small pulse **s** [24, 25]. For the pulse **l**, $x_T^{\mathbf{l}} = 0.607255$ gives the non-zero eigenvalue $\lambda = -0.165986 < 0$, indicating it is stable. For the small pulse **s**, $x_T^{\mathbf{s}} = 0.21325$, gives $\lambda = 0.488339 > 0$ indicating it is unstable.

4. Computing the eigenvalues. For the case of $\alpha > 0$, we must compute the eigenvalues of (2.11) with the integral operator. Our strategy is to reduce the integral equation to a piecewise linear ODE on three separate regions. The discrete spectrum can then be obtained from the zeros of the determinant of a linear system based on the matching conditions between the regions. This approach is similar to the Evans function method [15, 16, 17, 18].

4.1. ODE form of the eigenvalue problem. We transform (2.11) (with the connection function defined by (1.3)) into three piecewise linear ordinary differential equations (ODEs) on $(-\infty, x_{T_1})$, $(-x_{T_1}, x_{T_1})$ and $(-x_{T_1}, \infty)$. The ODEs then obey a set of matching conditions at $x = x_{T_1}$ and $x = -x_{T_1}$.

On the domain $x \in (-x_{T_1}, x_{T_1})$, we can write (2.11) in the form

$$(1+\lambda)v(x) = T_1(x) + I_1 - I_2 + I_3 - I_4 \tag{4.1}$$

where

$$I_1(x) = \alpha \int_{-x_{T_1}}^{x} A e^{-a(x-y)} v(y)dy, \qquad I_2(x) = \alpha \int_{-x_{T_1}}^{x} e^{-(x-y)} v(y)dy$$
$$I_3(x) = \alpha \int_{x}^{x_{T_1}} A e^{a(x-y)} v(y)dy, \qquad I_4(x) = \alpha \int_{x}^{x_{T_1}} e^{(x-y)} v(y)dy$$

and

$$T_1(x) = w(x - x_{T_1})\frac{v(x_{T_1})}{c} + w(x + x_{T_1})\frac{v(-x_{T_1})}{c}. \tag{4.2}$$

Differentiating (4.1) repeatedly gives

$$(1+\lambda)v'(x) = T_1'(x) - aI_1 + I_2 + aI_3 - I_4 \tag{4.3}$$
$$(1+\lambda)v''(x) = T_1''(x) + a^2 I_1 - I_2 + a^2 I_3 - I_4 + 2\alpha(1 - aA)v(x) \tag{4.4}$$
$$(1+\lambda)v'''(x) = T_1'''(x) - a^3 I_1 + I_2 + a^3 I_3 - I_4 + 2\alpha(1 - aA)v'(x) \tag{4.5}$$
$$(1+\lambda)v''''(x) = T_1''''(x) + a^4 I_1 - I_2 + a^4 I_3 - I_4 + 2\alpha(1 - a^3 A)v(x) + 2\alpha(1 - aA)v''(x) \tag{4.6}$$

where we have used

$$I_1' = -aI_1 + \alpha A v(x), \qquad I_2' = -I_2 + \alpha v(x)$$
$$I_3' = aI_3 - \alpha A v(x), \qquad I_4' = I_4 - \alpha v(x).$$

Taking (4.5) $- a^2$(4.1) and rearranging gives

$$I_2 + I_4 = \frac{1}{a^2-1}\left[(\lambda+1)v'' + (2\alpha a A - 2\alpha - a^2\lambda - a^2)v + a^2 T_1 - T_1''\right]. \tag{4.7}$$

Substituting (4.7) back into (4.1) leads to

$$I_1 + I_3 = \frac{1}{a^2-1}\left[(\lambda+1)v'' + (2\alpha a A - 2\alpha - \lambda - 1)v + T_1 - T_1''\right]. \tag{4.8}$$

Substituting both (4.7) and (4.8) into (4.6), results in a fourth order ordinary differential equation for v on the domain $x \in (-x_T, x_T)$

$$\frac{1+\lambda}{\alpha}v'''' = \left[\frac{(1+\lambda)(a^2+1)}{\alpha} + 2(1-aA)\right]v'' + a\left[2(A-a) - \frac{\lambda+1}{\alpha}a\right]v + T_1''''(x) - (1+a^2)T_1''(x) + a^2 T_1(x). \tag{4.9}$$

Using $T_1''''(x) - (1+a^2)T_1''(x) + a^2 T_1(x) = 0$ (obtained by differentiating $T_1(x)$) and simplifying, leads to

$$(1+\lambda)v'''' - Bv'' + Cv = 0, \qquad x \in (-x_T, x_T) \tag{4.10}$$

where $B = (1+\lambda)(a^2+1) + 2\alpha(1-aA)$, and $C = (\lambda+1)a^2 - 2\alpha a(A-a)$.

On the domain $x \in (x_T, \infty)$, (2.11) can be written as

$$(1+\lambda)v = T_1 + J_1 - J_2, \tag{4.11}$$

where

$$J_1 = \alpha A \int_{-x_T}^{x_T} e^{-a(x-y)}v(y)dy, \qquad J_2 = \int_{-x_T}^{x_T} e^{-(x-y)}v(y)dy,$$

and T_1 is defined by (4.2) on the domain (x_T, ∞).

Differentiating (4.11) and using $J_1' = -aJ_1$ and $J_2' = -J_2$ gives

$$(1+\lambda)v'(x) = T_1' - aJ_1 + J_2, \tag{4.12}$$

$$(1+\lambda)v''(x) = T_1'' + a^2 J_1 - J_2. \tag{4.13}$$

Taking a(4.11)+$(a+1)$(4.12)+(4.13) and using $T_1'' + (1+a)T_1' + aT_1 = 0$ leads to

$$v'' + (a+1)v' + av = 0, \qquad x \in (x_T, \infty). \tag{4.14}$$

Similarly, the ODE on $(-\infty, -x_T)$ is given by

$$v'' - (a+1)v' + av = 0, \qquad x \in (-\infty, -x_T). \tag{4.15}$$

In summary, the eigenvalue problem (2.11) reduces to three ODEs:

(ODE I)	$v'' - (a+1)v' + av = 0,$	$x \in (-\infty, -x_T),$
(ODE II)	$(1+\lambda)v'''' - Bv'' + Cv = 0,$	$x \in (-x_T, x_T),$
(ODE III)	$v'' + (a+1)v' + av = 0,$	$x \in (x_T, \infty),$

where $B = (1+\lambda)(a^2+1) + 2\alpha(1-aA)$ and $C = (\lambda+1)a^2 - 2\alpha a(A-a)$.

4.2. Matching Conditions. The solutions of ODE I, II, and III and their first three derivatives must satisfy a set of matching conditions across the boundary points $-x_T$ and x_T. We derive these conditions from the original eigenvalue equation (2.11) which we write as

$$c(1+\lambda)v(x) = w(x-x_T)v(x_T) + w(x+x_T)v(-x_T) + c\alpha W(x), \tag{4.16}$$

where $W(x) = \displaystyle\int_{-x_T}^{x_T} w(x-y)v(y)dy$, $x \in (-\infty,\infty)$. From (4.16), we see that $v(x)$ is continuous on $(-\infty,\infty)$. However, $w(x)$ has a cusp at $x=0$ which will lead to discontinuities in the derivatives of $v(x)$ across the boundary points $-x_T$ and x_T.

We first probe the discontinuities of $W(x)$ and its derivatives. $W(x)$ is continuous on $(-\infty,\infty)$. By a change of variables, $W(x) = \int_{x-x_T}^{x+x_T} w(z)v(x-z)dz$, from which we obtain

$$W'(x) = w(x+x_T)v(-x_T) - w(x-x_T)v(x_T) + \int_{x-x_T}^{x+x_T} w(z)v'(x-z)dz,$$

indicating that $W'(x)$ is also continuous on $(-\infty,\infty)$. However $W'(x)$ is not smooth at $-x_T$ and x_T. Differentiating $W'(x)$ for $x \neq -x_T, x_T$ gives

$$\begin{aligned} W''(x) &= w'(x+x_T)v(-x_T) - w'(x-x_T)v(x_T) + w(x+x_T)v'(-x_T^+) \\ &\quad - w(x-x_T)v'(x_T^-) - \int_{x+x_T}^{x-x_T} w(z)v''(x-z)dz \end{aligned}$$

where $v'(-x_T^+) = \lim\limits_{x\to -x_T^+} v'(x)$ for $x > -x_T$ (right limit) and $v'(x_T^-) = \lim\limits_{x\to x_T^-} v'(x)$ for $x < x_T$ (left limit).

Using the following convention:

$$[\cdot]\,|_{x=x_T} = \cdot|_{x=x_T^+} - \cdot|_{x=x_T^-} \qquad [\cdot]\,|_{x=-x_T} = \cdot|_{x=-x_T^+} - \cdot|_{x=-x_T^-}$$

to represent the jump at the boundaries, we find that

$$\begin{aligned} [W''(x_T)] &= W''(x)|_{x=x_T^+} - W''(x)|_{x=x_T^-} = -[w'(0)]\,v(x_T) \\ [W''(-x_T)] &= W''(x)|_{x=-x_T^+} - W''(x)|_{x=-x_T^-} = [w'(0)]\,v(-x_T) \end{aligned}$$

We differentiate $W''(x)$ for $x \neq -x_T, x_T$ and find

$$\begin{aligned} [W'''(x_T)] &= -[w''(0)]\,v(x_T) - [w'(0)]\,v'(x_T^-) \\ [W'''(-x_T)] &= [w''(0)]\,v(-x_T) + [w'(0)]\,v'(-x_T^+) \end{aligned}$$

To find the matching conditions for the derivatives of $v(x)$, we differentiate (4.16) with respect to x for $x \neq -x_T, x_T$, and obtain

$$c(1+\lambda)v'(x) = w'(x-x_T)v(x_T) + w'(x+x_T)v(-x_T) + c\alpha W'(x).$$

$v'(x)$ is discontinuous at the boundaries because of the discontinuity of $w'(x)$ at $x=0$. Therefore

$$\begin{aligned} [v'(x_T)] &= \frac{1}{c(1+\lambda)}\,[w'(0)]\,v(x_T), \\ [v'(-x_T)] &= \frac{1}{c(1+\lambda)}\,[w'(0)]\,v(-x_T). \end{aligned}$$

Differentiating (4.16) twice yields

$$c(1+\lambda)v''(x) = w''(x-x_T)v(x_T) + w''(x+x_T)v(-x_T) + c\alpha W''(x) \qquad x \neq -x_T, x_T$$

There are discontinuities of $v''(x)$ at $-x_T$ and x_T that come from $W''(-x_T)$ and $W''(x_T)$. Note that $w''(0^-) = w''(0^+)$. The jump conditions of $v''(x)$ at $-x_T$ and x_T are

$$\begin{aligned}
[v''(x_T)] &= \frac{\alpha}{1+\lambda}[W''(x_T)] = -\frac{\alpha}{1+\lambda}[w'(0)]\,v(x_T),\\
[v''(-x_T)] &= \frac{\alpha}{1+\lambda}[W''(-x_T)] = \frac{\alpha}{1+\lambda}[w'(0)]\,v(-x_T).
\end{aligned}$$

By differentiating a third time we find the jump conditions for $v'''(x)$ at $-x_T$ and x_T:

$$\begin{aligned}
[v'''(x_T)] &= \frac{1}{c(1+\lambda)}[w'''(0)]\,v(x_T) + \frac{\alpha}{1+\lambda}[W'''(x_T)]\\
&= \frac{1}{c(1+\lambda)}[w'''(0)]\,v(x_T) - \frac{\alpha}{1+\lambda}[w'(0)]\,v'(x_T^-),\\
[v'''(-x_T)] &= \frac{1}{c(1+\lambda)}[w'''(0)]\,v(-x_T) + \frac{\alpha}{1+\lambda}[W'''(x_T)]\\
&= \frac{1}{c(1+\lambda)}[w'''(0)]\,v(-x_T) + \frac{\alpha}{1+\lambda}[w'(0)]\,v'(-x_T^+)
\end{aligned}$$

Using the connection function $w(x)$ defined in (1.3), we have

$$\begin{aligned}
[w'(0)] &= w'(0^+) - w'(0^-) = 2(1-aA)\\
[w''(0)] &= w''(0^+) - w''(0^-) = 0\\
[w'''(0)] &= w'''(0^+) - w'''(0^-) = 2(1-a^3A)
\end{aligned}$$

These results lead directly to the following theorem.

THEOREM 4.1. *The continuous eigenfunction $v(x)$ on $(-\infty,\infty)$ in (2.11) has the following jumps in its first, second and third order derivatives at the boundary $-x_T$ and x_T.*

$$[v(x_T)] = 0 \tag{4.17}$$

$$[v'(x_T)] = \frac{2\alpha(1-aA)}{1+\lambda}v(x_T) \tag{4.18}$$

$$[v''(x_T)] = \frac{2(aA-1)}{c(1+\lambda)}v(x_T) \tag{4.19}$$

$$[v'''(x_T)] = \frac{2(1-a^3A)}{c(1+\lambda)}v(x_T) + \frac{2\alpha(aA-1)}{1+\lambda}v'(x_T^-) \tag{4.20}$$

$$[v(-x_T)] = 0 \tag{4.21}$$

$$[v'(-x_T)] = \frac{2\alpha(1-aA)}{1+\lambda}v(-x_T) \tag{4.22}$$

$$[v''(-x_T)] = \frac{-2(aA-1)}{c(1+\lambda)}v(-x_T) \tag{4.23}$$

$$[v'''(-x_T)] = \frac{2(1-a^3A)}{c(1+\lambda)}v(-x_T) - \frac{2\alpha(aA-1)}{1+\lambda}v'(-x_T^+). \tag{4.24}$$

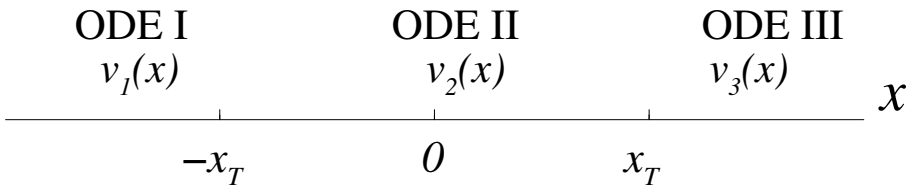

FIG. 4.1. *Valid ODEs on different sections and their solutions*

4.3. Eigenfunction symmetries. We define $v_1(x)$, $v_2(x)$ and $v_3(x)$ as the solutions of ODE I, ODE II and ODE III, respectively (see Fig. 4.1.) The three ODEs are all linear with constant coefficients. The continuous and bounded eigenfunction $v(x)$ of (2.11) is defined as the following

$$v(x) = \begin{cases} v_1(x), & x \in (-\infty, -x_T], \\ v_2(x), & x \in [-x_T, x_T], \\ v_3(x), & x \in [x_T, \infty), \end{cases}$$

and $v_1(x)$ matches $v_2(x)$ at $-x_T$ and $v_2(x)$ matches $v_3(x)$ at x_T.

LEMMA 4.2. *The eigenfunction $v(x)$ is either even or odd.*

Proof. By symmetry of ODE II, if $v_2(x)$ is a solution then $v_2(-x)$ is also a solution Hence, both the even function $\dfrac{v_2(x)+v_2(-x)}{2}$ and the odd function $\dfrac{v_2(x)-v_2(-x)}{2}$ are solutions of ODE II.

Let

$$T_2(x) = \alpha \int_{-x_T}^{x_T} w(x-y)v_2(y)dy.$$

If $v_2(x)$ is an even function, then since $w(x)$ is even, $T_2(x)$ is also even.

By the continuity of $v(x)$ on $\Re$, $v(x_T)$ and $v(-x_T)$ can be replaced by $v_2(x_T^-)$ and $v_2(-x_T^+)$, respectively. Thus the eigenvalue problem (2.11) is

$$(1+\lambda)v(x) = w(x-x_T)\frac{v_2(x_T)}{c} + w(x+x_T)\frac{v_2(-x_T)}{c} + T_2(x) \tag{4.25}$$

Given that $v_2(x)$, $w(x)$ and $T_2(x)$ are all even functions, from (4.25), we see that $v(x)$ is also even. Similar, we can show that $v(x)$ is odd when $v_2(x)$ is odd. □

LEMMA 4.3. *The matching conditions at $-x_T$ are identical to those at x_T when $v(x)$ is an odd or an even function.*

Proof. This is shown with a direct calculation of the matching conditions of $v'(x)$, $v''(x)$ and $v'''(x)$ at both $-x_T$ and x_T.

If $v(x)$ is even, *i.e.* $v(-x_T) = v(x_T)$ and $v'(-x_T^+) = -v'(x_T^-)$, then defining the jump of v at x as $[v(x)] = v(x^+) - v(x^-)$, the follow equalities are derived

$$[v(-x_T)] = -[v(x_T)] \tag{4.26}$$

$$[v'(-x_T)] = [v'(x_T)] \tag{4.27}$$

$$[v''(-x_T)] = -[v''(x_T)] \tag{4.28}$$

$$[v'''(-x_T)] = [v'''(x_T)] \tag{4.29}$$

Given the equalities (4.26)-(4.29), a direct calculation shows that the matching conditions (4.21)-(4.24) at $-x_T$ are equivalent to the matching conditions (4.17)-(4.20) at x_T.

When $v(x)$ is odd, using the same approach, we can also justify that the matching conditions at $-x_T$ and x_T are the same. □

4.4. ODE Solutions. ODEs I, II, and III are linear with constant coefficients and can be readily solved in terms of the parameters A, a, α, and u_T. The eigenvalue λ is specified when the solutions of the three ODEs are matched across the boundaries at $x = -x_T$ and $x = x_T$. Solutions of ODE I are related to ODE III by a reflection $x \to -x$. By Lemma 4.3, the matching conditions at $-x_T$ are the same as those at x_T. Thus matching solutions $v_2(x)$ of ODE II with solutions $v_3(x)$ of ODE III across x_T are sufficient to specify the eigenvalues of (2.11). The solution of ODE III is

$$v_3(x) = c_5 e^{-ax} + c_6 e^{-x},$$

where c_5 and c_6 are constants. Notice that $v_3(x)$ exponentially decays to zero as $x \to \infty$, in accordance with the assumed properties of $v(x)$.

The solutions of ODE II will depend nontrivially on the parameters A, a, and α. The characteristic equation of ODE II is

$$(1+\lambda)\omega^4 - B\omega^2 + C = 0,$$

where

$$B = (1+\lambda)(a^2+1) + 2\alpha(1-aA) \tag{4.30}$$

and

$$C = (1+\lambda)a^2 - 2\alpha a(A-a). \tag{4.31}$$

The characteristic values are

$$\omega^2 = \frac{B \pm \sqrt{\Delta}}{2(1+\lambda)} \tag{4.32}$$

where

$$\begin{aligned} \Delta &= B^2 - 4(1+\lambda)C \\ &= (a^2-1)^2\lambda^2 + 2(a^2-1)(a^2-1-2aA\alpha-2\alpha)\lambda - \\ &\quad (a^2-1)(1-a^2+4\alpha+4aA\alpha) + 4\alpha^2(1-aA)^2 \end{aligned} \tag{4.33}$$

Let λ_B be the zero of B. If Δ is negative, (4.32) shows that ODE II will have complex characteristic values. If Δ is positive, combinations of B and Δ yield either real or imaginary values. For fixed A, a and α, Δ is a parabola with a left zero λ_l and a right zero λ_r. By Lemma (8.9) and Lemma (8.10) in the Appendix, either $\lambda_l \le \lambda_B \le \lambda_r$ and does not intersect with either branch of $\sqrt{\Delta}$ or $\lambda_B \le \lambda_l$ and intersects with the left branch of $\sqrt{\Delta}$. Table 4.1 and 4.2 describe all the possible structures of the characteristic values $\pm\omega_1$ and $\pm\omega_2$. There are three possible forms of solution $v_2(x)$: 1) both ω_1 and ω_2 are real; 2) both ω_1 and ω_2 are complex; 3) ω_1 is real and ω_2 is imaginary.

We notate the even solutions of ODE II as $v_2^{\mathrm{e}}(x)$ and the odd solutions as $v_2^{\mathrm{o}}(x)$. When $\lambda \ge \lambda_r$ or $\lambda_I \le \lambda \le \lambda_l$, both ω_1 and ω_2 are real. Thus

$$v_2^{\mathrm{e}}(x) = c_3\mu_1(x) + c_4\frac{\mu_1(x)-\mu_2(x)}{\omega_1-\omega_2} \tag{4.34}$$

TABLE 4.1
Characteristic value chart when $\lambda_l < \lambda_B < \lambda_r$

1	2	3	4	5
$-1 < \lambda < \lambda_l$	$\lambda = \lambda_l$	$\lambda_l < \lambda < \lambda_r$	$\lambda = \lambda_r$	$\lambda > \lambda_r$
$B < 0$	$B < 0$	$B > 0$ or $B < 0$	$B > 0$	$B > 0$
$\Delta > 0$, $\lvert B\rvert < \sqrt{\Delta}$	$\Delta = 0$	$\Delta < 0$	$\Delta = 0$	$\Delta > 0$
ω_1 real ω_2 imaginary	$\omega_{1,2}$ imaginary $\omega_1 = \omega_2^*$	$\omega_{1,2}$ complex $\omega_1 = \omega_2^*$	$\omega_{1,2}$ real $\omega_1 = \omega_2$	$\omega_{1,2}$ real

TABLE 4.2
Characteristic value chart when $\lambda_B < \lambda_l < \lambda_r$

1	2	3	4	5	6
$-1 < \lambda < \lambda_I$	$\lambda_I \le \lambda < \lambda_l$	$\lambda = \lambda_l$	$\lambda_l < \lambda < \lambda_r$	$\lambda = \lambda_r$	$\lambda > \lambda_r$
$B < 0$ or $B > 0$	$B > 0$	$B > 0$	$B < 0$	$B > 0$	$B > 0$
$\Delta > 0$, $\lvert B\rvert < \sqrt{\Delta}$	$\Delta > 0$, $\lvert B\rvert > \sqrt{\Delta}$	$\Delta = 0$	$\Delta < 0$	$\Delta = 0$	$\Delta > 0$
ω_1 real ω_2 imaginary	$\omega_{1,2}$ real	$\omega_{1,2}$ real $\omega_1 = \omega_2$	$\omega_{1,2}$ complex $\omega_1 = \omega_2^*$	$\omega_{1,2}$ real $\omega_1 = \omega_2$	$\omega_{1,2}$ real

where $\mu_1(x) = e^{\omega_1 x} + e^{-\omega_1 x}$, and $\mu_2(x) = e^{\omega_2 x} + e^{-\omega_2 x}$. We use (4.34) because it is more convenient to resolve the degenerate case of $\omega_1 = \omega_2$. As $\lambda \to \lambda_r^-$, $\mu_1 \to \mu_2$ and $\epsilon = \omega_1 - \omega_2 \to 0$, (4.34) becomes

$$v_2^{\mathrm{e}}(x) = = c_3(e^{\omega_1 x} + e^{-\omega_1 x}) + c_4 \frac{(e^{\omega_1 x} + e^{-\omega_1 x}) - (e^{\omega_1 x} e^{-\epsilon x} + e^{-\omega_1 x} e^{\epsilon x})}{\epsilon}$$

Replacing $e^{\epsilon x}$ by $1 + \epsilon x$, $e^{-\epsilon x}$ by $1 - \epsilon x$ and taking the limit as $\epsilon \to 0$ yields

$$\begin{aligned} v_2^{\mathrm{e}}(x) &= c_3(e^{\omega_1 x} + e^{-\omega_1 x}) + c_4 x(e^{\omega_1 x} - e^{-\omega_1 x}) \\ &= 2c_3 \cosh px + 2c_4 x \sinh px \end{aligned} \tag{4.35}$$

(4.34) approaches (4.35) as $\lambda \to \lambda_r^-$. It matches the solution $v_2^{\mathrm{e}}(x)$ as $\lambda \to \lambda_r^+$, which is given in (4.37).

Similarly, $v_2^{\mathrm{o}}(x)$ can be written as

$$v_2^{\mathrm{o}}(x) = c_3(e^{\omega_1 x} - e^{-\omega_1 x}) + c_4 \frac{(e^{\omega_1 x} - e^{-\omega_1 x}) - (e^{\omega_2 x} - e^{-\omega_2 x})}{\omega_1 - \omega_2}$$

When $\lambda_l < \lambda < \lambda_r$, ω_1 and ω_2 are complex. Let $\omega_1 = p + iq$, $\omega_2 = p - iq$. When $v_2(x)$ is even, write $v_2^{\mathrm{e}}(x)$ as

$$v_2^{\mathrm{e}}(x) = 2c_3 \cos qx \cosh px + 2c_4 \frac{\sin qx}{q} \sinh px \tag{4.36}$$

As $\lambda \to \lambda_l^+$ or λ_r^-, $q \to 0$,

$$v_2^{\mathrm{e}}(x) \to 2c_3 \cosh px + 2c_4 x \sinh px \tag{4.37}$$

$v_2^o(x)$ can be written as

$$v_2^o(x) = 2c_3 \cos qx \sinh px - 2c_4 \frac{\sin qx}{q} \cosh px$$

where $p = \sqrt{\frac{\sqrt{B^2+|\Delta|}}{2(1+\lambda)}} \cos\theta$, $p = \sqrt{\frac{\sqrt{B^2+|\Delta|}}{2(1+\lambda)}} \sin\theta$ and $\theta = \frac{1}{2} \arctan \frac{\sqrt{|\Delta|}}{B}$.

When $-1 < \lambda < \lambda_I$, ω_1 is real and w_2 is imaginary. Let $\omega_2 = iq$, where $q = \sqrt{\frac{\sqrt{\Delta} - B}{2(1+\lambda)}}$, then

$$v_2^e(x) = c_3(e^{\omega_1 x} + e^{-\omega_1 x}) + 2c_4 \cos(qx) \tag{4.38}$$

$$v_2^o(x) = c_3(e^{\omega_1 x} - e^{-\omega_1 x}) + 2c_4 \frac{\sin(qx)}{q} \tag{4.39}$$

5. Stability criteria. By theorem 4.1, $v_1(x)$ and $v_2(x)$ must match at $-x_T$, and $v_2(x)$ and $v_3(x)$ must match at x_T. By property 4.3, the matching conditions at $-x_T$ are same as the matching conditions at x_T for $v(x)$ even or odd. Therefore, it suffices to apply the matching condition to $v_2(x)$ and $v_3(x)$ at x_T for the even and odd cases separately. This reduces the dimensionality of the resulting eigenvalue problem by a factor of two. In general, the matching conditions can be written as

$$T1: \begin{cases} [v(x_T)] = v_3(x_T^+) - v_2(x_T^-) & = & 0 \\ [v'(x_T)] = v_3'(x_T^+) - v_2'(x_T^-) & = & \frac{2\alpha(1-aA)}{1+\lambda} v(x_T) \\ [v''(x_T)] = v_3''(x_T^+) - v_2''(x_T^-) & = & \frac{2(aA-1)}{c(1+\lambda)} v(x_T) \\ [v'''(x_T)] = v_3'''(x_T^+) - v_2'''(x_T^-) & = & \frac{2(1-a^3A)}{c(1+\lambda)} v(x_T) + \frac{2\alpha(aA-1)}{1+\lambda} v'(x_T^-) \end{cases}$$

where $v(x_T) = v_3(x_T^+)$ and $v'(x_T^-) = v_2'(x_T^-)$.

A given stationary pulse solution $u_0(x)$ will be specified by a set of parameters a, A, α, x_T, and u_T. The eigenvalues λ that determine stability of pulse solutions are given by system T1. To compute these eigenvalues, we require the appropriate form of the eigenfunctions $v_2(x)$ and $v_3(x)$. We do so by finding characteristic values (4.32) corresponding to the parameters specifying the given stationary pulse solution. We expediate this process by calculating the constants B (4.30) and C (4.31), then using Table 4.1 and Table 4.2 to deduce the characteristic value types. We then substitute the appropriate form for $v_2(x)$ and $v_3(x)$ into T_1 where coefficients c_3 and c_4 in $v_2(x_T)$ and c_5 and c_6 in $v_3(x_T)$ are unknown. We replace $v(x_T)$ by $v_3(x_T^+)$ and $v'(x_T^-)$ by $v_2'(x_T^-)$. This results in a 4×4 homogeneous linear system with 4 unknown free parameters c_3, c_4, c_5, c_6. We must do this for both even and odd eigenfunctions resulting in two separate linear systems that must be solved.

The coefficient matrix of this system must be singular for a non-trivial solution (c_3, c_4, c_5, c_6). Hence, the determinant $D(\lambda)$ of the coefficient matrix must be zero. Thus, the solution of $D(\lambda) = 0$ is an eigenvalue and it determines the stability of the stationary solution. If there exists a λ such that $0 < \lambda < \lambda_b$ and $D(\lambda) = 0$, then the standing pulse is unstable. If there is no positive λ such that $0 < \lambda < \lambda_b$ and $D(\lambda) = 0$, the standing pulse is stable. Our determinant $D(\lambda)$ for stability is similar to the Evans Function [15, 16, 17, 18].

5.1. Stability of the small and large pulse. Two single-pulse solutions were shown to exist in the accompanying paper [24] for parameters $a = 2.4$, $A = 2.8$, $\alpha = 0.22$, $u_T = 0.400273$ and $\beta = 1$. The large pulse has a higher amplitude and larger width and is denoted by $u^{\mathbf{l}}(x)$. The small pulse is slightly above threshold and much narrower than $u^{\mathbf{l}}(x)$ and is denoted by $u^{\mathbf{s}}(x)$. The explicit forms are given by

$$u^{\mathbf{l}}(x) = \begin{cases} 0.665\cos(0.31x)\cosh(1.49x) - 3.78\sin(0.31x)\sinh(1.49x) + 0.33, & x \in [-x_T, x_T] \\ 6.237e^{-2.4|x|} - 1.604e^{-|x|}, & \text{otherwise} \end{cases}$$

where $x_T = 0.683035$.

$$u^{\mathbf{s}}(x) = \begin{cases} 0.22\cos(0.31x)\cosh(1.49x) - 8.03\sin(0.31x)\sinh(1.49x) + 0.33, & x \in [-x_T, x_T] \\ 1.203e^{-2.4|x|} - 0.416e^{-|x|}, & \text{otherwise} \end{cases}$$

where $x_T = 0.202447$.

We first calculate the upper bound for the eigenvalue λ_b which is different for the large pulse and small pulse because λ_b depends on x_T. Let $\lambda_b^{\mathbf{l}}$ be the upper bound for the large pulse and $\lambda_b^{\mathbf{s}}$ be the upper bound for the small pulse. For the parameter set $a = 2.4, A = 2.8, \alpha = 0.22, u_T = 0.400273$, the upper bounds are $\lambda_b^{\mathbf{l}} = 1.25917$ and $\lambda_b^{\mathbf{s}} = 1.66628$.

For the above set of parameters, $v_3(x)$ always has the following form.

$$v_3(x) = c_5 e^{-ax} + c_6 e^{-x}.$$

The form of $v_2(x)$ depends on ω_1 and ω_2. For this specific set of parameters, the left and right solutions of Δ (4.33) are $\lambda_l = -0.627692$ and $\lambda_r = 0.192861$. When $0 \le \lambda \le \lambda_r$, both ω_1 and ω_2 are complex, implying

$$v_2(x) = \begin{cases} v_2^{\mathrm{e}}(x) = 2c_3\cos qx\cosh px + 2c_4\dfrac{\sin qx}{q}\sinh px & v_2(x) \text{ is even} \\ v_2^{\mathrm{o}}(x) = 2c_3\cos qx\sinh px - 2c_4\dfrac{\sin qx}{q}\cosh px & v_2(x) \text{ is odd} \end{cases}$$

where p, q are real, and c_3, c_4 are unknown.

Substituting $v_2^{\mathrm{e}}(x)$ ($v_2^{\mathrm{o}}(x)$) and $v_3(x)$ into system $T1$, results in an unwieldy 4×4 linear system in c_3, c_4, c_5 and c_6. We use Mathematica [55] to calculate the determinant of the coefficient matrix as a function of λ.

When $0.192861 = \lambda_r \le \lambda \le \lambda_b^{\mathbf{l}} = 1.25917$, $\omega_{1,2}$ is real, and $v_2(x)$ has the form

$$v_2(x) = \begin{cases} c_3(e^{\omega_1 x} + e^{-\omega_1 x}) + c_4\dfrac{(e^{\omega_1 x} + e^{-\omega_1 x}) - (e^{\omega_2 x} + e^{-\omega_2 x})}{\omega_1 - \omega_2} & v_2(x) \text{ is even} \\ c_3(e^{\omega_1 x} - e^{-\omega_1 x}) - c_4\dfrac{(e^{\omega_1 x} - e^{-\omega_1 x}) - (e^{\omega_2 x} + e^{-\omega_2 x})}{\omega_1 - \omega_2} & v_2(x) \text{ is odd} \end{cases}$$

Figure 5.1 gives a plot of $D(\lambda)$ on the domain $[0, \lambda_b]$, combining the regimes where $\omega_{1,2}$ is real and complex. We see that there is no positive λ that satisfies $D(\lambda) = 0$. Figure 5.2 shows $D(\lambda)$ for odd $v(x)$. We see that $D(\lambda) = 0$ only when $\lambda = 0$, which is consistent with Theorem 8.6. The lack of a positive zero of $D(\lambda)$ indicates that the large pulse is stable.

For the same set of parameters, $\{a = 2.4, A = 2.8, \alpha = 0.22, u_T = 0.400273\}$, the upper bound of the small pulse is $\lambda_b^{\mathbf{s}} = 1.66628$ Repeating the same procedure as for the large pulse, we plot $D(\lambda)$ for both $v_2^{\mathrm{e}}(x)$ and $v_2^{\mathrm{o}}(x)$ (Figs 5.3 and 5.4). The existence of a positive eigenvalue $\lambda = \lambda^*$ satisfying $D(\lambda^*) = 0$ in Fig. 5.3 implies the instability of the small single-pulse. The plot of $D(\lambda)$ corresponding to $v^{\mathrm{o}}(x)$ in figure 5.4 identifies the zero eigenvalue.

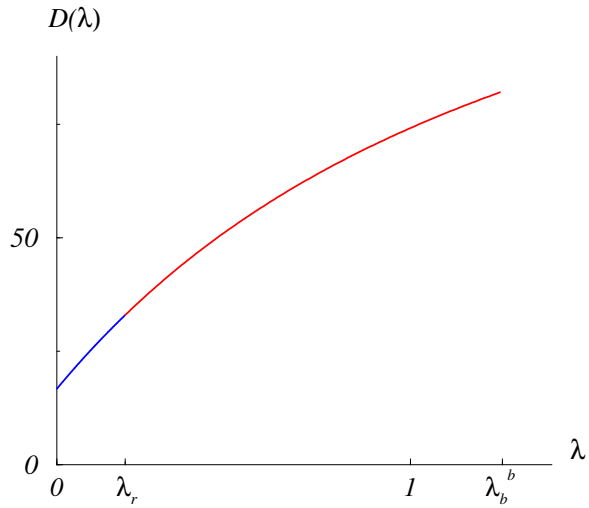

FIG. 5.1. *Plot of $D(\lambda)$ for large single-pulse $u^1(x)$ when $v_2(x)$ is even.* $a = 2.4$, $A = 2.8$, $\alpha = 0.22$, $u_T = 0.400273$, $x_T = 0.683035$, $\lambda_r = 0.192861$, $\lambda_b^1 = 1.25917$. *There is no positive λ such that $D(\lambda) = 0$, $\lambda \leq \lambda_b^1$.*

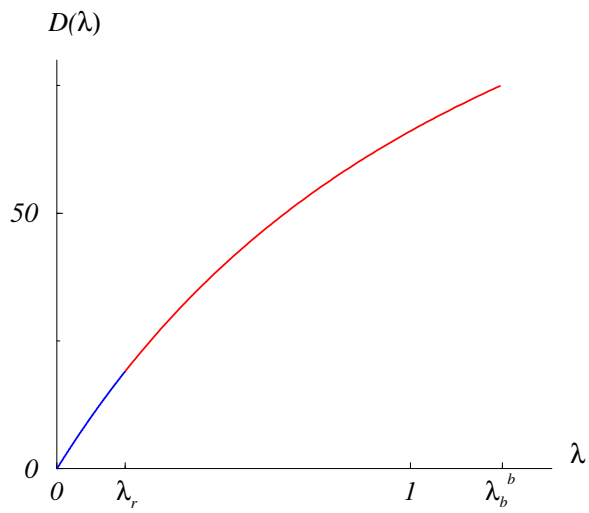

FIG. 5.2. *Plot of $D(\lambda)$ for large single-pulse $u^1(x)$ when $v_2(x)$ is odd.* $a = 2.4$, $A = 2.8$, $\alpha = 0.22$, $u_T = 0.400273$, $x_T = 0.683035$, $\lambda_r = 0.192861$, $\lambda_b^1 = 1.25917$. *There is no positive λ such that $D(\lambda) = 0$, $\lambda \leq \lambda_b^1$. When $v_2(x)$ is odd, $D(\lambda)$ does identify the zero eigenvalue.*

5.2. Stability and instability of for different gain α. For both the large single-pulses and small single-pulses, $D(\lambda)$ is monotonically increasing (See Fig 5.5 and 5.6). However, $D(0)$ for small pulses is negative. As λ increases, $D(\lambda)$ crosses the λ-axis and becomes positive. Therefore, $D(\lambda)$ has a positive zero. For the large pulse, $D(0)$ is positive and $D(\lambda)$ has no positive zero. We follow $D(0)$ for a range of $\alpha \in (0.22, 0.59)$ in Fig 5.7 and find that $D(0)$ is always negative for small pulses and positive for large pulses. Hence, the large pulses are stable and the small pulses are unstable in this range.

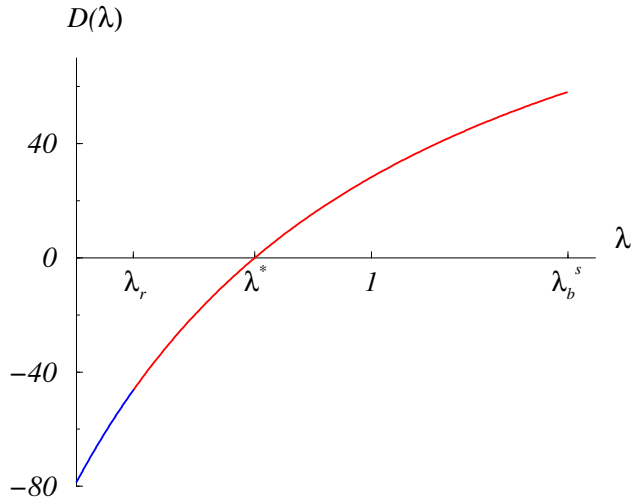

FIG. 5.3. *Plot of $D(\lambda)$ for small single-pulse $u^{\mathbf{s}}(x)$ when $v_2(x)$ is even. $a = 2.4$, $A = 2.8$, $\alpha = 0.22$, $u_T = 0.400273$, $x_T = 0.683035$, $\lambda_r = 0.192861$, $\lambda_b^{\mathbf{s}} = 1.66628$. $\lambda^* = 0.603705$ There is one positive $\lambda = \lambda^*$ such that $D(\lambda^*) = 0$, $\lambda^* \leq \lambda_b^{\mathbf{s}}$.*

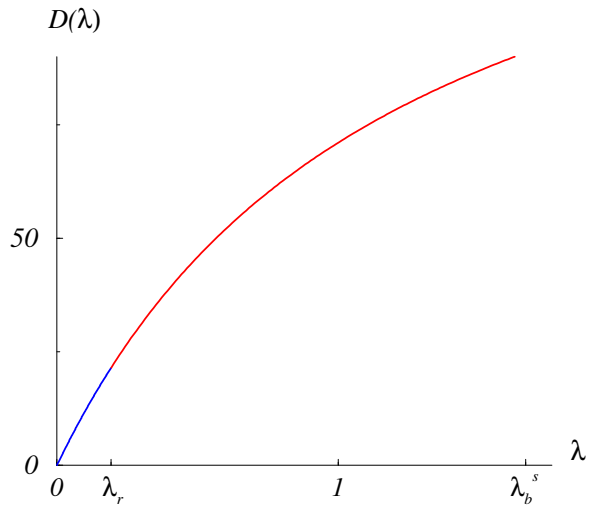

FIG. 5.4. *Plot of $D(\lambda)$ for small single-pulse $u^{\mathbf{s}}(x)$ when $v_2(x)$ is odd. $a = 2.4$, $A = 2.8$, $\alpha = 0.22$, $u_T = 0.400273$, $x_T = 0.683035$, $\lambda_r = 0.192861$, $\lambda_b^{\mathbf{s}} = 1.66628$. There is no positive λ such that $D(\lambda) = 0$, $\lambda \leq \lambda_b^{\mathbf{s}}$. When $v_2(x)$ is odd, $D(\lambda) = 0$ at $\lambda = 0$ identifies the zero eigenvalue.*

5.3. Stability of the dimple-pulse $u^{\mathbf{d}}(x)$ and the instability of the third pulse. When there are only two single-pulses, the large pulse could be a dimple-pulse instead of a single-pulse. This dimple pulse has the same stability properties as a large pulse. The parameter set $a = 2.4$, $A = 2.8$, $\alpha = 0.22$, $u_T = 0.18$, and $x_T = 2.048246$ corresponds to a dimple pulse. Carrying out the stability calculation yields $D(\lambda)$ shown in Figs. 5.8 and 5.9. We see that there is no zero crossing and thus the dimple pulse is stable. This is true for all dimple pulses we tested in this category.

As shown in [24] and [25], for certain parameter regimes, there can be more than

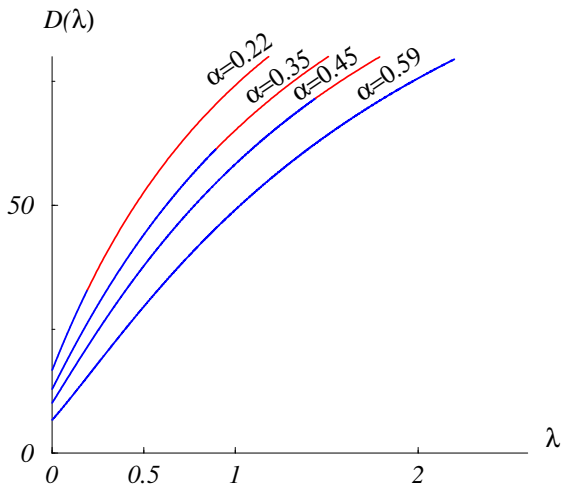

FIG. 5.5. *Plots of $D(\lambda)$ for large single-pulses with different gain α. $a = 2.4$, $A = 2.8$, $\alpha = 0.22$, $u_T = 0.400273$.*

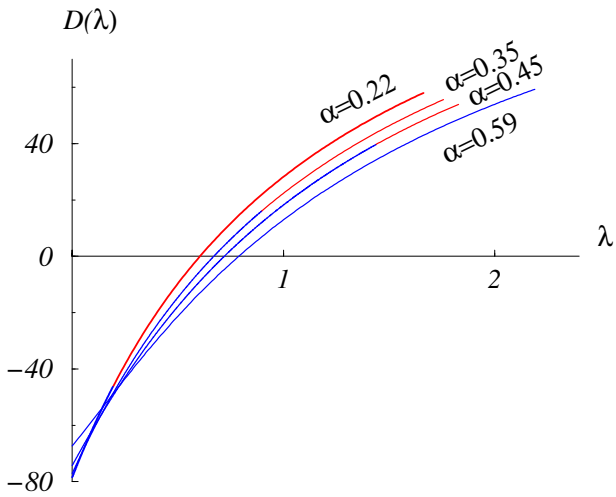

FIG. 5.6. *Plots of $D(\lambda)$ for small single-pulses with different gain α. $a = 2.4$, $A = 2.8$, $\alpha = 0.22$, $u_T = 0.400273$.*

two coexisting pulses. When there are three pulses, the third pulse can be either a single-pulse or a dimple-pulse. For example, when $A = 2.8$, $a = 2.2$, $\alpha = 0.8$, $u_T = 0.2$, the third pulse is the single-pulse

$$u(x)=\begin{cases}1.28\cos(0.47x)\cosh(1.2x)+1.27\sin(0.47x)\sinh(1.2x)+0.8129, & x\in[-x_T,x_T]\\ 198.78e^{2|x|}-15.15e^{-|x|}, & \text{otherwise}\end{cases}$$

where $x_T = 2.20629$. $D(\lambda)$ shown in Fig. 5.10 indicates that this pulse is unstable. When $a = 2.6$, $A = 2.8$, $\alpha = 0.6178$, $u_T = 0.063$, the third pulse is the dimple pulse

$$u(x)=\begin{cases}0.35\cos(1.112x)\cosh(1.112x)+0.24\sin(1.112x)\sinh(1.112x)+0.163, & x\in[-x_T,x_T]\\ 232.89e^{2.6|x|}-9.31e^{-|x|}, & \text{otherwise}\end{cases}$$

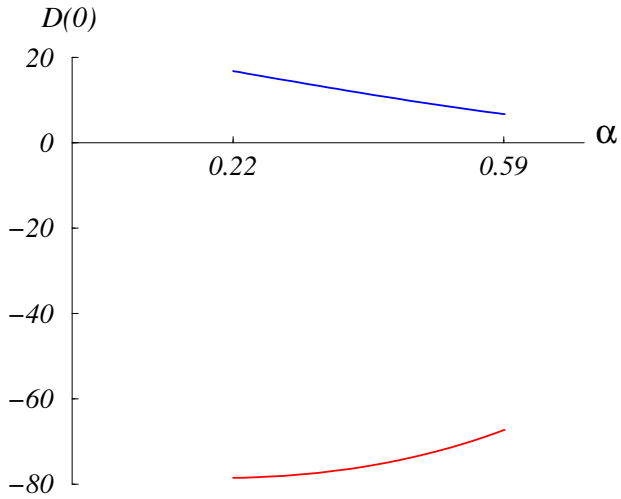

FIG. 5.7. *Plots of $D(0)$ for both large single-pulses (blue branch) and small single-pulse (red branch) with $\alpha \in (0.22, 0.59)$. $a = 2.4$, $A = 2.8.$, $u_T = 0.400273$.*

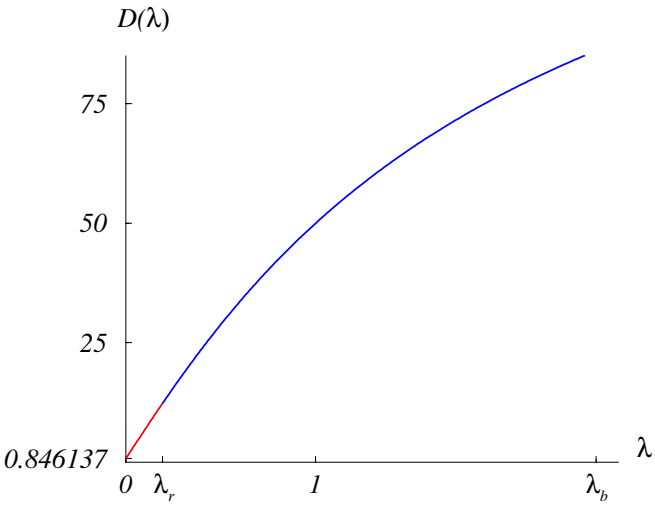

FIG. 5.8. *Plot of $D(\lambda)$ for dimple-pulse when $v_2(x)$ is even $a = 2.4$, $A = 2.8$, $\alpha = 0.22$, $x_T = 2.048246$, $\lambda_r = 0.192861$, $\lambda_b^{\mathbf{d}} = 2.48147$. There is no positive λ such that $D(\lambda) = 0$.*

where $x_T = 1.98232$. As seen in Fig. 5.11, $D(\lambda)$ crosses zero for a positive λ indicating that it is unstable. In all the cases that we have examined, we find that the third pulse is unstable.

6. Double-pulse and its stability. For certain parameter regimes, there can be double-pulse solutions which have two disjoint open and finite intervals for which the synaptic input $u(x)$ is above threshold [24, 25, 32]. An example is shown in Fig. 6.1). We consider symmetric double-pulses that satisfy the equation

$$u(x) = \int_{-x_2}^{x_1} w(x-y) f[u(y)]dy + \int_{x_1}^{x_2} w(x-y) f[u(y)]dy \tag{6.1}$$

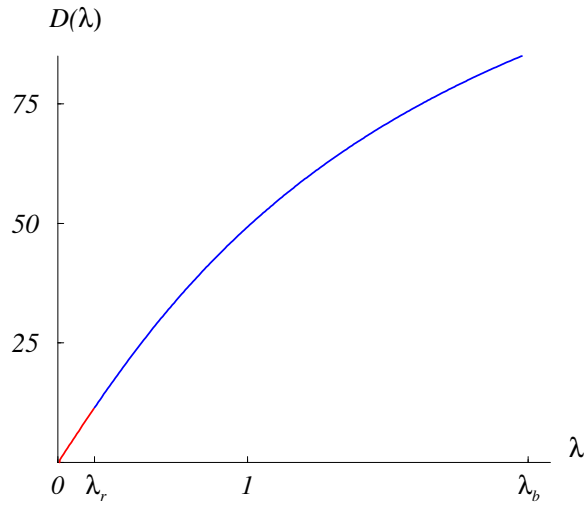

FIG. 5.9. *Plot of $D(\lambda)$ for dimple-pulse when $v_2(x)$ is odd.* $a = 2.4$, $A = 2.8$, $\alpha = 0.22$, $u_T = 0.18$, $x_T = 2.048246$, $\lambda_r = 0.192861$, $\lambda_b^{\mathbf{s}} = 2.48147$. *There is no positive λ such that $D(\lambda) = 0$, $\lambda \leq \lambda_b^{\mathbf{d}}$. When $v_2(x)$ is odd, $D(\lambda)$ does identify the zero eigenvalue because $D(\lambda) = 0$ at $\lambda = 0$. This is consistent with theorem.*

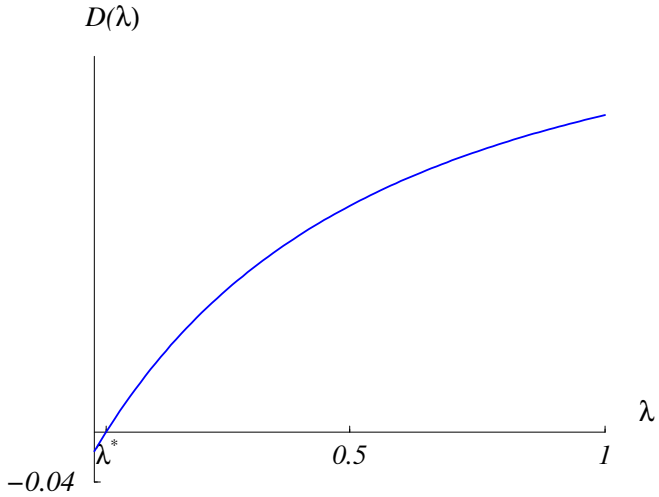

FIG. 5.10. *Plot of $D(\lambda)$ for the third pulse (a single-pulse) when $v_2(x)$ is even.* $a = 2.2$, $A = 2.8$, $\alpha = 0.8$, $u_T = 0.2$, $x_T = 2.0629$, $c = 2.75017$, $D(0) = -0.0153$. *There is a positive λ such that $D(\lambda) = 0$.*

where $x_{1,2} > 0$. Thus $u > u_T$ for $x \in (x_1, x_2) \cup (-x_2, -x_1)$, $u = u_T$ for $x = -x_2, -x_1, x_1, x_2$, and $u < u_T$ outside of these regions and approaches zero as $x \to \infty$. We show their existence in [24] and [25].

Linearizing the dynamical neural field equation (1.1) around a stationary double-pulse solution $u(x)$ gives eigenvalue equation:

$$(1+\lambda)v(x) = w(x-x_1)\frac{v(x_1)}{c_1} + w(x+x_1)\frac{v(-x_1)}{c_1} + w(x-x_2)\frac{v(x_2)}{c_2} \tag{6.2}$$

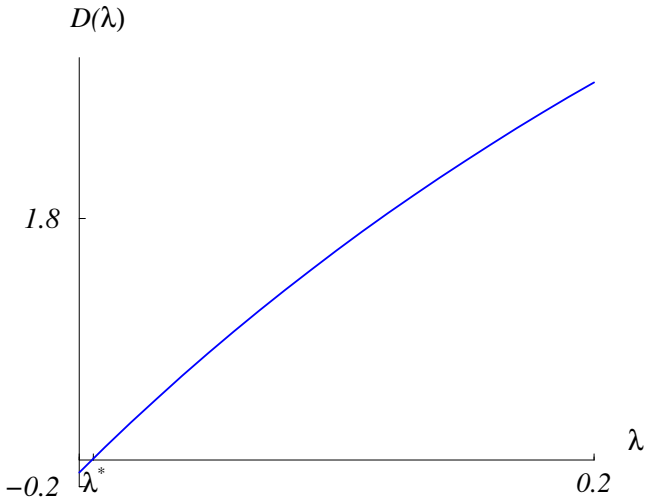

FIG. 5.11. *Plot of $D(\lambda)$ for the third pulse (a dimple-pulse) when $v_2(x)$ is even.* $a = 2.6$, $A = 2.8$, $\alpha = 0.6178$, $u_T = 0.063$, $x_T = 1.98232$, $c = 2.21523$, $D(0) = -0.094$. *There is a positive λ such that $D(\lambda) = 0$.*

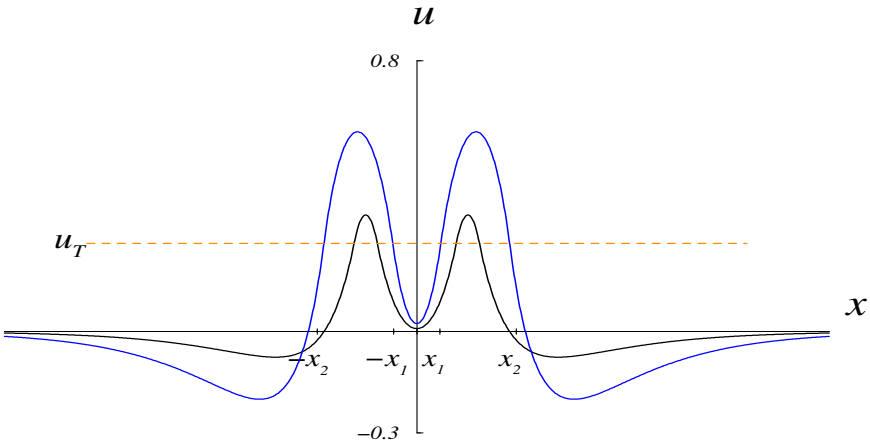

FIG. 6.1. *Double-pulse for Amari case in which $\alpha = 0$.* $A = 2.8$, $a = 2.6$, $\alpha = 0$, $u_T = 0.26$, $x_1 = 0.279525$, $x_2 = 1.20521$.

$$+ w(x + x_2)\frac{v(-x_2)}{c_2} + \alpha\left(\int_{-x_2}^{-x_1} w(x-y)v(y)dy + \int_{x_1}^{x_2} w(x-y)v(y)dy\right)$$

The eigenvalues λ of (6.2) possess the same properties as those of the eigenvalue equation for the single-pulse solutions.

For simplicity, we consider the Amari case in which $\alpha = 0$. The solution of (6.2) for $\alpha > 0$ would involve a long calculation. For $\alpha = 0$, the eigenvalue equation (6.2) becomes

$$(1+\lambda)v(x) = w(x-x_1)\frac{v(x_1)}{c_1} + w(x+x_1)\frac{v(-x_1)}{c_1} \tag{6.3}$$
$$w(x-x_2)\frac{v(x_2)}{c_2} + w(x+x_2)\frac{v(-x_2)}{c_2}$$

where $c_1 = u'(x_1)$ and $c_2 = u'(-x_2)$. Then $u'(-x_1) = -c_1$ and $u'(x_2) = -c_2$. Using an approach similar to Theorem 8.4 in the Appendix, we can show that λ is real. By taking the derivative of (6.1), we can also show that zero is an eigenvalue of system (6.3), and the corresponding eigenfunction is $u'(x)$.

Setting $x = x_1$, $x = -x_1$, $x = x_2$ and $x = -x_2$ in (6.3) gives a 4-dimensional system

$$\begin{pmatrix} \frac{w(0)-\lambda-1}{c_1} & \frac{w(2x_1)}{c_1} & \frac{w(x_1-x_2)}{c_2} & \frac{w(x_1+x_2)}{c_2} \\ \frac{w(2x_1)}{c_1} & \frac{w(0)-1-\lambda}{c_1} & \frac{w(x_1+x_2)}{c_2} & \frac{w(x_1-x_2)}{c_2} \\ \frac{w(x_1-x_2)}{c_1} & \frac{w(x_1+x_2)}{c_1} & \frac{w(0)-1-\lambda}{c_2} & \frac{w(2x_2)}{c_2} \\ \frac{w(x_1+x_2)}{c_1} & \frac{w(x_1-x_2)}{c_1} & \frac{w(2x_2)}{c_2} & \frac{w(0)-1-\lambda}{c_2} \end{pmatrix} \begin{pmatrix} v(x_1) \\ v(-x_1) \\ v(x_2) \\ v(-x_2) \end{pmatrix} = 0 \tag{6.4}$$

The determinant $D(\lambda)$ of coefficient matrix in system (6.4) is a fourth order polynomial. Since zero is an eigenvalue, then $D(\lambda) = \lambda d(\lambda)$, where $d(\lambda)$ is a third order polynomial. Consequently, the stability of the stationary solution $u(x)$ is determined by the roots of a third order polynomial $d(\lambda)$, which can be found numerically. We computed $d(\lambda)$ for the two double pulses shown in Fig. 6.1. Figure 6.2 shows a plot of the third order polynomial $d(\lambda)$ for the small double-pulse. It has three positive zeros indicating instability. The plot of $d(\lambda)$ for the large double-pulse as shown in Fig. 6.3) has two positive zeros. Therefore, both the small and large double-pulses are unstable. We have not found any stable double-pulses for any parameter sets that we tested. However, we have not fully investigated the parameter space of A, a and u_T.

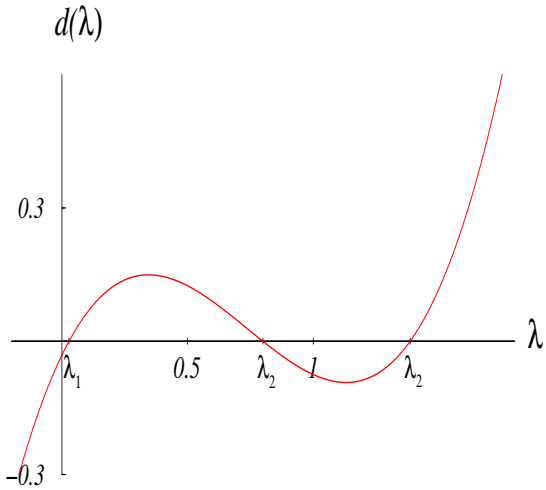

FIG. 6.2. *Plot of polynomial $d(\lambda)$ for the small double-pulse shown in Fig. 6.1.*

7. Discussion. Our results show that although many types of pulse-solutions are possible, only the family of large pulses and associated dimple pulses are stable. For the situation of three coexisting pulses, the third and largest pulse is always

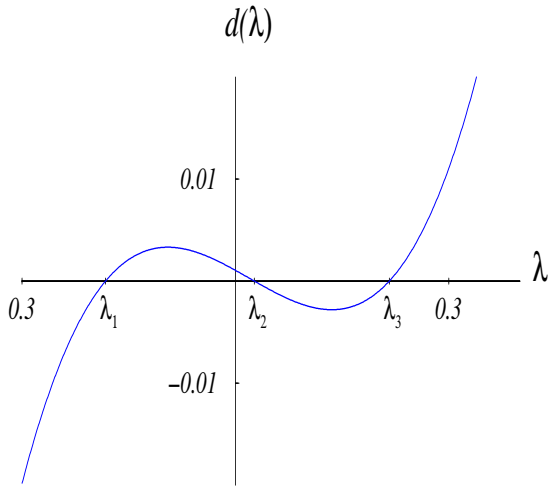

FIG. 6.3. *Plot of polynomial $d(\lambda)$ for the large double-pulse shown in Fig 6.1.*

unstable. It is possible that more than three pulses can coexist although we did not investigate situations beyond three. The double pulses we examined were not stable in accordance with previous work [32].

The caveat is that we were only able to examine specific examples individually or over limited parameter ranges. Although we have an analytical expression for the eigenvalues the length of these expressions makes them difficult to analyze. As a result, we were unable to make as strong a claim as Amari who showed that large pulses are always stable and small pulses are always unstable [3]. It may be possible to find some patterns in the expressions to make more general deductions. From our parameter explorations, we were unable to find stable pulse solutions other than the large and associated dimple pulse.

We wish to note that numerical simulations on discretized lattices can give misleading results regarding the stability and existence of pulse solutions of the associated continuum neural field equation. We conducted some numerical experiments using a discretization of the neural field equation (1.1) and to our surprise we were able to easily find examples of stable dimple and double pulses even though the continuum analogue shows that these solutions either do not exist or cannot be stable. The resolution to this paradox is that a discrete lattice may stabilize solutions that are marginally stable in the continuum case.

Consider the Amari neural network equation consisting of N neurons

$$\frac{du_i}{dt} = \Delta x \sum_{j=0}^{N} w(\Delta x(i-j))\Theta[u_j - u_T], \tag{7.1}$$

where $w(i-j)$ is given by (1.3), $\Theta(\cdot)$ is the Heaviside function, and Δx gives the discretization mesh size. For an initial condition for which $u_j > u_T$ on a contiguous set of points $\{i...k\}$ and $k-i$ is less than the expected width of the large pulse in the analogous continuum neural field equation, the numerical solution converges towards the expected large pulse solution. However, if the initial set of points is larger than the width of the large pulse (we have not fully investigated how much larger it needs to be), then there is a possibility that the simulation will converge towards an entirely different state.

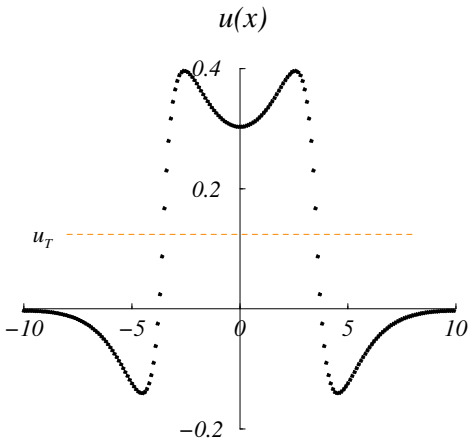

FIG. 7.1. *Result of numerical simulation of (7.1) for parameters* $N = 200$, $\Delta x = 0.1$, $A = 1.8$, $a = 1.6$, *and* $u_T = 0.124$. *The arbitrary discretization length scale is chosen so that* $x = 0.1i$.

For example, a numerical simulation of the parameter set $N = 200$, $\Delta x = 0.1$, $A = 1.8$, $a = 1.6$, and $u_T = 0.124$ with an initial condition $u_i = 1$ for $i \in 50...150$, converges to a stable dimple-pulse state shown in Fig. 7.1. Different initial domains will lead to different attracting states where the width is close to the initial domain width. For a large enough initial domain, the dimple pulse will break into a stable double-pulse. Increasing the initial domain can lead to increasingly higher number stable multiple pulses.

We can show that these states do not exist in the analogous continuum neural field equation Consider a stationary pulse solution of (1.1) for $\alpha = 0$. A pulse of width x_T satisfies

$$u(x) = \phi(x, x_T), \tag{7.2}$$

where

$$\phi(x, x_T) = \int_{-x_T}^{x_T} Ae^{-a|x-y|} - e^{-|x-y|} dy. \tag{7.3}$$

The pulse can exist if it satisfies the existence condition

$$u_T = \phi(x_T, x_T) \tag{7.4}$$

from which the width x_T can be obtained. A plot of the existence condition is shown in Fig. 7.2.

It is immediately apparent that the large pulse does not exist. The existence function approaches $u = u_T$ from above for large enough x_T. While it is very close to u_T it never crosses it. However, for the analogous discretized equation (7.1), the discrete mesh can break the symmetry of this nearly marginal mode and result in a family of stable pulse solutions for arbitrary widths larger than a given width.

This effect can be intuitively understood by examining Fig. 7.1. The neurons immediately adjacent to the edge of the pulse are significantly below threshold and thus have no effect on the rest of the network. A perturbation on the order of the distance they are below threshold would be necessary to cause these neurons to fire and influence the network. In the continuum equation, the neurons on the boundary of

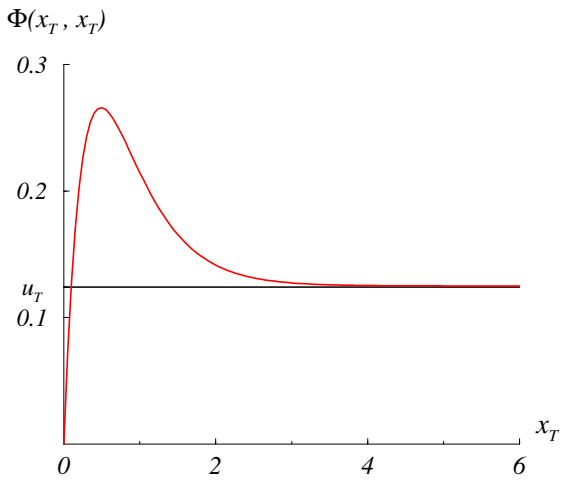

FIG. 7.2. *Existence condition for pulse solutions of neural field equation (7.2) for parameters* $A = 1.8$, $a = 1.6$, *and* $u_T = 0.124$.

the pulse are precisely at threshold. Arbitrarily small perturbations can push the field above threshold and influence the other neurons. A stable pulse must withstand these edge perturbations. Discretization eliminates these destabilizing edge perturbation effects.

We can make a simple estimate of how fine the discretization mesh must be in order for these discrete affects to disappear. The distance the neuron adjacent to the pulse is below threshold is approximately given by $\partial_x \phi(x = x_T, x_T)dx \sim (A-1)dx$. For the parameter set of our simulation, the continuum existence condition shows that $\phi(x_T, -x_T) - u_T > 0.001$. Thus to eliminate the discreteness effect, we require the adjacent neuron to be above threshold. i.e. $(A-1)dx < 0.001$ as it would be in the continuum case. This leads to an estimate of $dx < 0.00125$. Hence, for a domain of dimension $x > 20$, a network size of $N > 16,000$ is necessary to eliminate the discreteness effect.

Biological neural networks are inherently discrete. Thus this discreteness effect may be exploited by the brain to stabilize localized excitations. Our numerical simulation is an example of a discretized line attractor [51] where the width of the pulse is determined by the initial condition. Although, the discrete network may have a richer structure, this does not imply that the study of continuum neural field equations are not necessary. Field equations lend themselves more readily to analysis and many insights into the structure and properties of neural networks have been gained by studying them. We suggest that studies combining neural field equations, discrete neural network equations and biophysically based spiking neurons may be a fruitful way to uncover the dynamics of these systems.

8. Appendix 1: Properties of the eigenvalue problem. We prove some properties of the the eigenvalue problem (2.11) with the connection function given by (1.3). First consider functions

$$\phi_1(x) = \frac{1}{2a}\int_{-\infty}^{\infty} e^{-a|x-y|}(F_u + \Theta_u)v(y)dy$$

$$\phi_2(x) = \frac{1}{2}\int_{-\infty}^{\infty} e^{-|x-y|}(F_u + \Theta_u)v(y)dy$$

where $F(u) = \alpha(u - u_T)$, $\Theta(u)$ is the Heaviside function, and subscript denotes partial differentiation.

LEMMA 8.1. *The eigenfunction $v(x)$ satisfies*

$$(1+\lambda)v = 2(aA\phi_1 - \phi_2)$$

Proof.

$$\begin{aligned}
(1+\lambda)v &= w(x-x_T)\frac{v(x_T)}{c} + w(x+x_T)\frac{v(-x_T)}{c} + \alpha\int_{-x_T}^{x_T} w(x-y)v(y)dy \\
&= \int_{-\infty}^{\infty} w(x-y)\frac{\delta(x-x_T)+\delta(x+x_T)}{c}v(y)dy + \int_{-\infty}^{\infty} w(x-y)F_u v(y)dy \\
&= \int_{-\infty}^{\infty} w(x-y)\Theta_u v(y)dy + \int_{-\infty}^{\infty} w(x-y)F_u v(y)dy \\
&= A\int_{-\infty}^{\infty} e^{-a|x-y|}(F_u+\Theta_u)v(y)dy - \int_{-\infty}^{\infty} e^{-|x-y|}(F_u+\Theta_u)v(y)dy \\
&= 2(aA\phi_1 - \phi_2)
\end{aligned}$$

□

LEMMA 8.2. *Functions ϕ_1 and ϕ_2 satisfy*

$$-\phi_1'' + a^2\phi_1 = (F_u + \Theta_u)v \tag{8.1}$$

$$-\phi_2'' + a^2\phi_2 = (F_u + \Theta_u)v \tag{8.2}$$

Proof. The second order derivative of $\phi_1(x)$ is

$$\begin{aligned}
\phi_1'' = \frac{a}{2}\left[\int_{-\infty}^{x} e^{-a(x-y)}(F_u+\Theta_u)vdy + \int_{x}^{\infty} e^{a(x-y)}(F_u+\Theta_u)vdy\right] \\
- (F_u+\Theta_u)v
\end{aligned} \tag{8.3}$$

$-(8.3) + a^2\phi_1(x)$ yields

$$-\phi_1'' + a^2\phi_1 = (F_u + \Theta_u)v. \tag{8.4}$$

$-\phi_2'' + a^2\phi_2 = (F_u + \Theta_u)v$ can be obtained in the same fashion. □

LEMMA 8.3. $\lim_{x\to\pm\infty}\phi_{1,2} = 0$ *and* $\lim_{x\to\pm\infty}\phi_{1,2}' = 0$ *provided that $v(x)$ is bounded on $(-\infty,\infty)$ and exponentially decays to zero as $x \to \pm\infty$*

Proof. When $x >> x_T$

$$\phi_1(x) = \frac{1}{2a}\left[\alpha e^{-ax}\int_{-x_T}^{x_T} e^{ay}v(y)dy + e^{-a(x-x_T)}\frac{v(x_T)}{c} + e^{-a(x+x_T)}\frac{v(-x_T)}{c}\right].$$

Hence, $\lim_{x\to\infty}\phi_1 = 0$ provided that $v(x)$ is bounded on $[-x_T, x_T]$.

When $x << -x_T < 0$, as $x \to -\infty$

$$\phi_1(x) = \frac{1}{2a}\left[\alpha e^{ax}\int_{-x_T}^{x_T} e^{-ay}v(y)dy + e^{a(x-x_T)}\frac{v(x_T)}{c} + e^{a(x+x_T)}\frac{v(-x_T)}{c}\right] \to 0$$

$$\phi_1' = \frac{1}{2}\left[-\int_{-\infty}^{x} e^{-a(x-y)}(F_u+\Theta_u)v\,dy + \int_{x}^{\infty} e^{a(x-y)}(F_u+\Theta_u)v\,dy\right]$$

As $x \to \infty$,

$$\begin{aligned}\lim_{x\to\infty}\phi_1' &= \lim_{x\to\infty}\left\{-\frac{1}{2}\int_{-\infty}^{x} e^{-a(x-y)}(F_u+\Theta_u)v\,dy\right\}\\ &= \lim_{x\to\infty}\left\{-\frac{e^{-ax}}{2}\left[\alpha\int_{-x_T}^{x_T} e^{ay}dy + e^{ay}\frac{v(x_T)}{c}\right]\right\} = 0\end{aligned}$$

As $x \to -\infty$

$$\begin{aligned}\lim_{x\to-\infty}\phi_1' &= \lim_{x\to-\infty}\left\{-\frac{1}{2}\int_{x}^{\infty} e^{a(x-y)}(F_u+\Theta_u)v\,dy\right\}\\ &= \lim_{x\to\infty}\left\{-\frac{e^{ax}}{2}\left[\alpha\int_{-x_T}^{x_T} e^{ay}dy + e^{ax_T}\frac{v(x_T)}{c}\right]\right\} = 0\end{aligned}$$

Similarly, one can prove that $\lim_{x\to\pm\infty}\phi_2 = 0$ and $\lim_{x\to\pm\infty}\phi_2' = 0$. Therefore, $\lim_{x\to\pm\infty}\phi_{1,2} = 0$ and $\lim_{x\to\pm\infty}\phi_{1,2}' = 0$. □

THEOREM 8.4. *The eigenvalue λ in (2.11) is always real.*

Proof. Using the results of Lemma 8.2, $aA\bar{\phi}_1(8.1) - \bar{\phi}_2(8.2)$ gives

$$aA\bar{\phi}_1(-\phi_1'' + a^2\phi_1) - \bar{\phi}_2(-\phi_2'' + \phi_2) = (F_u+\Theta_u)v(aA\bar{\phi}_1 - \bar{\phi}_2) \tag{8.5}$$

where $\bar{\phi}_{1,2}$ are the complex conjugates of $\phi_{1,2}$. Integration by parts gives

$$\int_{-\infty}^{\infty}\bar{\phi}_1\phi_1''dx = \bar{\phi}_1\phi_1'|_{-\infty}^{\infty} - \int_{-\infty}^{\infty}\bar{\phi}_1'\phi_1'dx = -\int_{-\infty}^{\infty}|\phi_1'|^2\,dx$$

and similarly $\int_{-\infty}^{\infty}\bar{\phi}_2\phi_2''dx = -\int_{-\infty}^{\infty}|\phi_2'|^2\,dx$. ¿From Lemma 8.1

$$\begin{aligned}\frac{1}{2}(1+\lambda)v &= aA\phi_1 - \phi_2\\ \frac{1}{2}(1+\bar{\lambda})\bar{v} &= aA\bar{\phi}_1 - \bar{\phi}_2\end{aligned}$$

Integrating both sides of (8.5) gives

$$\begin{aligned}&aA\left(\int_{-\infty}^{\infty}|\phi_1'|^2\,dx + a^2\int_{-\infty}^{\infty}|\phi_1|^2\,dx\right) -\\ &\left(\int_{-\infty}^{\infty}|\phi_2'|^2\,dx + \int_{-\infty}^{\infty}|\phi_2|^2\,dx\right) = \frac{1}{2}(1+\bar{\lambda})\int_{-\infty}^{\infty}|v|^2(F_u+\Theta_u)dx\end{aligned} \tag{8.6}$$

Using

$$\int_{-\infty}^{\infty}|v|^2\,\Theta_u dx = \frac{1}{c}\int_{-\infty}^{\infty}|v|^2\left(\delta(x-x_T)+\delta(x+x_T)\right)dx = \frac{1}{c}\left(|v(x_T)|^2 + |v(-x_T)|^2\right)$$

in (8.7) and rearranging gives

$$\frac{1}{2}(1+\bar{\lambda}) = \frac{aA\left(\int_{-\infty}^{\infty}|\phi_1'|^2\,dx + a^2\int_{-\infty}^{\infty}|\phi_1|^2\,dx\right) - \left(\int_{-\infty}^{\infty}|\phi_2'|^2\,dx + \int_{-\infty}^{\infty}|\phi_2|^2\,dx\right)}{\int_{-\infty}^{\infty}F_u\,|v|^2\,dx + \frac{1}{c}\left(|v(x_T)|^2 + |v(-x_T)|^2\right)} \tag{8.7}$$

The right-hand side of (8.7) is real, therefore λ is real. □

THEOREM 8.5. *The eigenvalue λ in (2.11) is bounded by $\lambda_b \equiv \frac{2k_0}{c} + 2\alpha k_1 x_T - 1$ where k_0 is the maximum of $|w(x)|$ on $[0, 2x_T]$ and $|w(x-y)| \le k_1$ for all $(x,y) \in J \times J$, where $J = [-x_T, x_T]$.*

Proof. We write the eigenvalue problem (2.11) as

$$(1+\lambda)v = Lv \tag{8.8}$$

where operator L is defined as (2.12).

Function $w(x-y)$ is continuous on square $J \times J$. We take the norm of both sides of (8.8)

$$(1+\lambda)\|v\| = \|Lv\|$$

with norm

$$\|\cdot\| = \max_{x\in J}|\cdot|$$

Thus

$$\begin{aligned}
\|Lv\| &= \left\| w(x-x_T)\frac{v(x_T)}{c} + w(x+x_T)\frac{v(-x_T)}{c} + \alpha\int_{-x_T}^{x_T} w(x-y)v(y)dy \right\| \\
&\le \max_{x\in J}\left| w(x-x_T)\frac{v(x_T)}{c}\right| + \max_{x\in J}\left| w(x+x_T)\frac{v(-x_T)}{c}\right| + \\
&\qquad \max_{x\in J}\left|\alpha\int_{-x_T}^{x_T} w(x-y)v(y)dy\right| \\
&\le |w(x-x_T)|\,\frac{\|v\|}{c} + |w(x+x_T)|\,\frac{\|v\|}{c} + \alpha\,\|v\|\int_{-x_T}^{x_T}\max_{x\in J}|w(x-y)|\,dy \\
&\le 2k_0\frac{\|v(x)\|}{c} + 2\alpha k_1 x_T\|v(x)\|
\end{aligned}$$

where

$$k_0 = \max_{x\in J}|w(x-x_T)| = \max_{x\in J}|w(x+x_T)|$$

since $w(x)$ is symmetric and $|w(x-y)| \le k_1$ for all $(x,y) \in J \times J$. Therefore

$$(1+\lambda)\|v(x)\| = \|Lv(x)\| \le 2k_0\frac{\|v(x)\|}{c} + 2\alpha k_1 x_T\|v(x)\|$$

leading to

$$\lambda \le \frac{2k_0}{c} + 2\alpha k_1 x_T - 1 \equiv \lambda_b.$$

□

THEOREM 8.6. *$\lambda = 0$ is an eigenvalue.*

Proof. Consider the equilibrium equation

$$\begin{aligned} u(x) &= \int_{-\infty}^{\infty} w(x-y) f[u(y)] dy \\ &= \int_{-x_T}^{x_T} w(x-y) \left\{\alpha \left[u(y) - u_T\right] + 1\right\} dy \end{aligned} \tag{8.9}$$

where $u(x)$ is a stationary standing pulse solution. After a change of variables $p = x - y$, (8.9) becomes

$$u(x) = \int_{x-x_T}^{x+x_T} w(p) \left\{\alpha \left[u(x-p) - u_T\right] + 1\right\} dp \tag{8.10}$$

Differentiating (8.10) with respect to x yields

$$\begin{aligned} u'(x) &= w(x+x_T)\left[\alpha(u(-x_T) - u_T) + 1\right] - w(x-x_T)\left[\alpha(u(x_T) - u_T) + 1\right] \\ &\quad + \alpha \int_{x-x_T}^{x+x_T} w(p) u'(x-p) dp \end{aligned} \tag{8.11}$$

Since $u(-x_T) = u(x_T) u_T$ and $u'(-x_T) = c = -u'(x_T)$,

$$\begin{aligned} u'(x) &= w(x+x_T)\frac{u'(-x_T)}{c} - w(x-x_T)\frac{-u'(x_T)}{c} + \alpha \int_{x-x_T}^{x+x_T} w(p) u'(x-p) dp \\ &= w(x-x_T)\frac{u'(x_T)}{c} + w(x+x_T)\frac{u'(-x_T)}{c} + \alpha \int_{-x_T}^{x_T} w(x-y) u'(y) dy \end{aligned} \tag{8.12}$$

(8.12) is the eigenvalue problem (2.11) with eigenvalue λ satisfying $1+\lambda = 1$, resulting in $\lambda = 0$. The corresponding eigenfunction is $u'(x)$. Therefore, $\lambda = 0$ is an eigenvalue of (2.11) corresponding to eigenfunction $u'(x)$. ∎

THEOREM 8.7. *Consider the operator*

$$L = T_1 + T_2, \tag{8.13}$$

where

$$\begin{aligned} T_1(v(x)) &= w(x-x_T)\frac{v(x_T)}{c} + w(x+x_T)\frac{v(-x_T)}{c}, && T_1 : C\left[-x_T, x_T\right] \to C\left[-x_T, x_T\right] \\ T_2(v(x)) &= \alpha \int_{-x_T}^{x_T} w(x-y) v(y) dy, && T_2 : C\left[-x_T, x_T\right] \to C\left[-x_T, x_T\right] \end{aligned}$$

Both T_1 and T_2 and hence L are compact operators.

Proof. It is obvious that both T_1 and T_2 are linear operators. The boundedness of T_1 follow from

$$\begin{aligned} \|T_1 v\| &= \max_{x \in J} \left| w(x-x_T)\frac{v(x_T)}{c} + w(x+x_T)\frac{v(-x_T)}{c} \right| \\ &\le |w(x-x_T)| \frac{\|v(x)\|}{c} + |w(x+x_T)| \frac{\|v(x)\|}{c} \\ &\le 2k_0 \frac{\|v\|}{c} \end{aligned}$$

Let v_n be any bounded sequence in $C\left[-x_T, x_T\right]$ and $\|v_n\| \le c_0$ for all n. Let $y_n^1 = T_1 v_n$. Then $\|y_n^1\| \le \|T_1\| \|v_n\|$. Hence sequence y_n^1 is bounded. Since $w(x,t) = w(x-t)$ is

continuous on $J \times J$ and $J \times J$ is compact, w is uniformly continuous on $J \times J$. Hence, for any given $\epsilon_1 > 0$, there is a $\delta_1 > 0$ such that for $t = x_T$ and all $x_1, x_2 \in J$ satisfying $|x_1 - x_2| < \delta_1$

$$|w(x_1 - x_T) - w(x_2 - x_T)| < \frac{c}{2c_0}\epsilon_1.$$

Consequently, for x_1, x_2 as before and every n, one can obtain

$$\begin{aligned}
\left|y_n^1(x_1) - y_n^1(x_2)\right| &= \Big|[w(x_1 - x_T) - w(x_2 - x_T)]\,\frac{v_n(x_T)}{c} \\
&\quad + [w(x_1 + x_T) - w(x_2 + x_T)]\,\frac{v_n(-x_T)}{c}\Big| \\
&< |w(x_1 - x_T) - |w(x_2 - x_T)|\,\frac{c_0}{c} + |w(x_1 + x_T) - w(x_2 + x_T)|\,\frac{c_0}{c} \\
&< \frac{c}{2c_0}\epsilon_1\frac{c_0}{c} + \frac{c}{2c_0}\epsilon_1\frac{c_0}{c} = \epsilon_1
\end{aligned}$$

Boundedness of T_2 follows from

$$\|T_2 v\| \le \|v\| \max_{x \in J} \int_{-x_T}^{x_T} |w(x - t)|dt$$

Similarly, let $y_n^2 = T_2 v_n$. Then y_n^2 is bounded. For any given $\epsilon_2 > 0$, there is a $\delta_2 > 0$ such that for any $t \in J$ and all $x_1, x_2 \in J$ satisfying $|x_1 - x_2| < \delta_2$

$$|w(x_1 - t) - w(x_2 - t)| < \frac{\epsilon_2}{2x_T}$$

$$\begin{aligned}
\left|y_n^2(x_1) - y_n^2(x_2)\right| &= \left|\int_{-x_T}^{x_T} [w(x_1 - t) - w(x_2 - t)]v_n(t)dt\right| \\
&< 2x_T\frac{\epsilon_2}{2x_T c_0} = \epsilon_2
\end{aligned}$$

This proves the equicontinuity of $\{y_n^1\}$ and $\{y_n^2\}$. By Ascoli's theorem, both sequences have convergent subsequences. v_n is an arbitrary bounded sequence and $y_n^1 = T_1 v_n$, $y_n^2 = T_2 v_n$. The compactness of T_1 and T_2 follows from the criterion that an operator is compact if and only if it maps every bounded sequence x_n in X onto a sequence Tx_n in Y which has a convergent subsequence. □

THEOREM 8.8. *$\lambda = -1$ is the only possible accumulation point of the eigenvalues of L and every spectral value $\lambda \neq -1$ of L is an eigenvalue of L. Thus the only possible essential spectrum of compact operator L is at $\lambda = -1$.*

Proof. Let $\gamma = (1 + \lambda)$, the eigenvalue problem becomes

$$\gamma v(x) = Lv(x),$$

and the linear operator L is compact on the normed space $C[-x_T, x_T]$. γ is the eigenvalue of operator L. The spectrum of a compact operator is a countable set with no accumulation point different from zero. Each nonzero member of the spectrum is an eigenvalue of the compact operator with finite multiplicity [29, 28]. Therefore, the only possible point of accumulation for the spectrum set of compact operator L is $\gamma = 0$, *i.e.*, $\lambda = -1$ and every spectral value $\lambda \neq -1$ of L is an eigenvalue of L.

This suggests that the only possible essential spectrum is at $\lambda = -1$. All the spectral values λ such that $\lambda > -1$ are eigenvalues. □

LEMMA 8.9. *The zero of B, λ_B, obeys $-1 < \lambda_B < \lambda_r$. For the case $a^3 > A$, $\lambda_l < \lambda_B < \lambda_r$, and for the case $a^3 < A$, $\lambda_B < \lambda_l < \lambda_r$.*

Proof. Set

$$B = (1+\lambda)(a^2+1) + 2\alpha(1-aA) = 0$$

The zero of B is

$$\lambda_B = -\frac{a^2+1+2\alpha-2aA\alpha}{a^2+1} = -1 + \frac{2\alpha(aA-1)}{a^2+1} > -1.$$

Δ is a quadratic function in λ and it has two zeros. The left zero is

$$\lambda_l = \frac{1-a^2+2aA\alpha+2\alpha-4\alpha\sqrt{aA}}{a^2-1}$$

The right zero is

$$\lambda_r = \frac{1-a^2+2aA\alpha+2\alpha+4\alpha\sqrt{aA}}{a^2-1}$$

The difference between λ_r and λ_B is

$$\lambda_r - \lambda_B = \frac{4a\alpha(a+A)+4\alpha\sqrt{aA}(a^2+1)}{a^4-1} > 0$$

Therefore $-1 < \lambda_B < \lambda_r$.

The difference between λ_B and λ_l is $\lambda_B - \lambda_l = \dfrac{4\alpha(\sqrt{aA}-1)(a^2-\sqrt{aA})}{a^4-1}$. The sign of $\lambda_B - \lambda_l$ depends on $a^2 - \sqrt{aA}$. If $a^2 - \sqrt{aA}$ is positive, *i.e.* $a^3 > A$, then $\lambda_l < \lambda_B < \lambda_r$. If $a^2 - \sqrt{aA}$ is negative, *i.e.*, $a^3 < A$, then $\lambda_B < \lambda_l < \lambda_r$. □

LEMMA 8.10. *(i) For $a^3 > A$ and $\lambda_l < \lambda_B < \lambda_r$, B does not intersect the left branch or the right branch of $\sqrt{\Delta}$. (ii) For $a^3 < A$ and $\lambda_B < \lambda_l < \lambda_r$, B intersects only the left branch of $\sqrt{\Delta}$ once at λ_I.*

Proof. It is not difficult to see that B does not intersect the right branch of $\sqrt{\Delta}$ for both (i) and (ii). $\sqrt{\Delta}$ is linear in λ with slope a^2-1 for large λ. The slope of B is a^2+1. Both a^2-1 and a^2+1 are positive and $a^2+1 > a^2-1$, thus B and the right branch of $\sqrt{\Delta}$ never meet. When $\lambda_l < \lambda_B < \lambda_r$, $B < 0$ for $\lambda < \lambda_B$ and $\sqrt{\Delta} > 0$ for $\lambda < \lambda_l < \lambda_B$. Therefore B and $\sqrt{\Delta}$ never intersect. In (ii), B intersects the left branch of $\sqrt{\Delta}$ at $\lambda_I = \dfrac{2A\alpha - 2a\alpha - a}{a}$. □

Acknowledgments. We thank G. Bard Ermentrout, William Troy, Xinfu Chen, Jonathan Rubin, and Bjorn Sandestade for illuminating discussions. This work was supported by the National Institute of Mental Health, the A. P. Sloan foundation and the National Science Foundation under Agreement No. 0112050.

REFERENCES

[1] C. D. Aliprantis. *Problems in real analysis: a workbook with solutions.* Academic Press, 1999.
[2] C. D. Aliprantis and Burkinshaw. *Principles of real analysis.* Academic Press, 1998.

[3] S. Amari. Dynamics of pattern formation in lateral-inhibition type neural fields. *Biol. Cybernetics*, 27:77–87, 1977.
[4] M. A. Arbib, editor. *The Handbook of Brain Theory and Neural Networks*. MIT Press, 1995.
[5] K. E. Atkinson. *Numerical solution of integral equations of the second kind*. Cambridge University Press, 1997.
[6] C. M. Bender and S. A. Orszag. *Advanced mathematical methods for scientists and engineers I: Asyptotic methods and perturbation theory*. Springer, 1999.
[7] W. E. Boyce and R. C. DiPrima. *Introduction to differential equations*. John Wiley and Sons, 1970.
[8] A. R. Champneys and J. P. McKenna. On solitary waves of a piece-wise linear suspended beam model. *Nonlinearity*, 10:1763–1782, 1997.
[9] L. M. Delves and J. L. Mohamed. *Computational methods for integral equations*. Cambridge University Press, 1988.
[10] D. G. Duffy. *Green's functions with applications*. Chapman and Hall/CRC, 2001.
[11] S. A. Ellias and S. Grossberg. Pattern formation, contrast control, and oscillations in the short-term memory of shunting on-center off-surround networks. *Biol. Cybern.*, 20:69–98, 1975.
[12] G. B. Ermentrout. Xppaut, simulation software tool.
[13] G. B. Ermentrout. Neural networks as spatio-temporal pattern-forming systems. *Rep. Prog. Phys.*, 61:353–430, 1998.
[14] G. B Ermentrout. *Simulating, Analyzing, and Animating Dynamical Systems: A Guide to XPPAUT for Researchers and Students*. SIAM, 2002.
[15] J. W. Evans. Nerve axon equations, i: Linear approximations. *Indiana Univ. Math. J.*, 21:877–955, 1972.
[16] J. W. Evans. Nerve axon equations, ii: Stability at rest. *Indiana Univ. Math. J.*, 22:75–90, 1972.
[17] J. W. Evans. Nerve axon equations, iii: Stability of the nerve impulse. *Indiana Univ. Math. J.*, 22:577–594, 1972.
[18] J. W. Evans. Nerve axon equations, iv: The stable and unstable impulse. *Indiana Univ. Math. J.*, 24:1169–1190, 1975.
[19] G. B. Folland. *Fourier analysis and its applications*. Wadsworth and Brooks/Cole Advanced Books and Software, 1992.
[20] J. M Fuster. *Prefrontal cortex: anatomy, physiology, and neuropsychology of the frontal lobe*. Lippincott-Raven Publishers, 1997.
[21] F. Garvan. *The Maple Book*. Chapman and Hall, 2001.
[22] C. D. Green. *Integral equation methods*. Nelson, 1969.
[23] D. H. Griffel. *Applied functional analysis*. Ellis Horwood, 1985.
[24] Y. Guo. Existence and stability of standing pulses in neural networks. PhD thesis, University of Pittsburgh, 2003.
[25] Y. Guo and C.C. Chow. Existence and stability of standing pulses in neural networks: I. existence. Preprint, 2004.
[26] B.S. Gutkin, C.R. Laing, C. L. Colby, C.C. Chow, and G. B. Ermentrout. Turing on and off with excitation: the role of spike-timing asynchrony and synchrony in sustained neural activity. *J. Comp. Neurosci.*, 11:121–134, 2001.
[27] E Haskell and P. C. Bressloff. On the formation of persistent states in neuronal networks models of feature selectivity. *J. Integ. Neurosci.*, 2:103–123, 2003.
[28] T. Kato. *Perturbation theory for linear operators*. Springer, 1995.
[29] E. Kreyszig. *Introductory Functional Analysis with Applications*. John Wiley and Sons, 1978.
[30] Y. A. Kuznetsov. *Elements of applied bifurcation theory*. Springer, 1998.
[31] C. R. Laing and C. C. Chow. Stationary bumps in networks of spiking neurons. *Neural Comp.*, 13:1473–1493, 2001.
[32] C. R. Laing and W. C. Troy. Two-bump solutions of amari type models of working memory. *Physica D*, pages 190–218, 2003.
[33] C. R. Laing, w. C. Troy, B Gutkin, and G. B Ermentrout. Multiple bumps in a neuronal model of working memory. *SIAM J. of Applied Math.*, 63, no.1:62–97, 2002.
[34] C. R. Laing and William C. Troy. Pde methods for nonlocal models. *SIAM Journal on Applied*

Dynamical Systems, 2:487–516, 2001.

[35] E. K. Miller, C. A. Erickson, and R. Desimone. Neural mechanisms of visual working memory in prefrontal cortex of the macaque. *J. Neurosci.*, 16:5154–5167, 1996.

[36] N. Morrison. *Introduction to Fourier analysis.* Wiley-Interscience, 1994.

[37] J. D. Murray. *Mathematical biology.* Springer, 2002.

[38] J. G. Nicholls. *From neuron to brain: a cellular molecular approach to the function of the nervous system.* Sinauer Associates, 1992.

[39] Y. Nishiura and M. Mimura. Layer oscillations in reactoin-diffusion systems. *SIAM J. Appl. Math.*, 49:481–514, 1989.

[40] E. Pärt-Enander, A. Sjöberg, Melin B., and Isaksson P. *The MATLAB handbook.* Addison-Wesley, 1998.

[41] L. A. Peletier and W. C. Troy. *Spatial patterns: higher order models in physics and mechanics.* Birkhauser, 2001.

[42] E. Pelinovsky, D and V. G. Yakhno. Generation of collective-activity structures in a homogeneous neuron-like medium. i. bifurcation analysis of static structures,. *Bifurcation Chaos Appl. Sci. Eng.*, 6:81–87, 89–100, 1996a,b.

[43] J. D. Pinto and Ermentrout G. B. Spatially structured activity in synaptically coupled neuronal networks:2 lateral inhibition and standing pulses. *SIAM J. Appl. Math.*, 62:226–243, 2001.

[44] A. D. Polianin and A. V. Manzhirov. *Handbook of integral equations.* CRC Press, 1998.

[45] D. L. Powers. *Boundary value problems.* Harcourt Academic Press, 1999.

[46] M. Rahman. *Complex variables and transform calculus.* Computational Mechanics Publications, 1997.

[47] J. E. Rubin, D. Terman, and C. C. Chow. Localized bumps of activity sustained by inhibition in a two-layer thalamic network. *J Comp Neurosci*, 10:313–331, 2001.

[48] J. E Rubin and W. C Troy. Sustained spatial patterns of activity in neuronal populations with or without lateral inhibition. *SIAM J. Appl. Math.*, 2004.

[49] W. Rudin. *Principles of mathematical analysis.* McGraw-Hill, 1976.

[50] E. Salinas and L. F. Abbott. A model of multiplicative neural responses in parietal cortex. *Proc Natl Acad Sci USA*, 93:11956–11961, 1996.

[51] S. H. Seung. How the brain keeps the eyes still. *Proc Natl Acad Sci USA*, 93:13339–44, 1996.

[52] S. H. Strogatz. *Nonlinear dynamics and chaos.* Perseus Books, 1994.

[53] S. Wiggins. *Introduction to applied nonlinear dynamical systems and chaos.* Springer, 1990.

[54] H. R. Wilson and J. D. Cowan. A mathematical theory of the functional dynamics of cortical and thalamic nervous tissue. *Kybernetic*, 13:55–80, 1973.

[55] S. Wolfram. *The Mathematica Book.* Cambridge University Press, 4th Edition, 1999.

[56] E. Zeidler. *Nonlinear functional analysis and its applications I: fixed-point theorems.* Springer, 1986.